Pergamon

Int. J. Heat Mass Transfer. Vol. 39, No. 16, pp. 3381–3400, 1996

0017-9310/96 $15.00+0.00

PII: S0017-9310(96)00025-7

Flow transitions and combined free and forced convective heat transfer in a rotating curved circular tube

LIQIU WANG† and K. C. CHENG

Department of Mechanical Engineering, University of Alberta, Edmonton, Alberta, Canada T6G 2G8

(*Received* 20 *June* 1995 *and in final form* 5 *December* 1995)

Abstract—The simultaneous effects of curvature, rotation and heating/cooling of the tube complicate the flow and heat transfer characteristics beyond those observed in the tubes with simple curvature, rotation or heating/cooling. The phenomena encountered are investigated for steady, hydrodynamically and thermally fully developed laminar flow in circular tubes. A full second-order perturbation solution is obtained under the condition that the wall heat flux is uniform with peripherally uniform wall temperature. The results cover both the nature of flow transitions and the effect of these transitions on temperature distribution, friction factor and Nusselt number. When the rotation is in the same direction as the main flow imposed by a pressure gradient and the fluid is heated, the flow and heat transfer remain similar to those observed in stationary curved tubes, radially rotating straight tubes or mixed convection in stationary straight tubes. There are, however, quantitative changes due to the combined effects of centrifugal, Coriolis and buoyancy forces. A more complex behaviour is possible when the rotation is opposite to the flow due to the pressure gradient or when the fluid is cooled. In particular, the inward Coriolis force and/or buoyancy force may cause the direction of the secondary flow to reverse. The flow reversal occurs by passing through a four-cell vortex flow region where overall, the centrifugal, Coriolis and buoyancy forces just neutralize each other. Copyright © 1996 Elsevier Science Ltd.

1. INTRODUCTION

Fluid flow and heat transfer in rotating curved channels are not only of considerable theoretical interest, but also of practical importance in many engineering applications [1, 2]. The curvature and rotation, in conjunction with heating or cooling, introduce the centrifugal force, the Coriolis force and the buoyancy force in the momentum equations which describe the relative motion of fluids with respect to the channel. Such body forces may induce a secondary flow in a plane perpendicular to the main flow. This could significantly affect the resistance to the fluid flow and convective heat transfer. As well, these forces may either enhance or impede each other in a nonlinear manner depending on the directions of the rotation and heat flux. This could result in a complicated structure of the flow. We examine this structure and its effects on flow resistance and convective heat transfer in the present study by a three-parameter perturbation method assuming the channel to be of a circular cross-section.

Works on the flows and heat transfer in a rotating curved channel are very limited. By employing Pohlhausen's method, Hocking [3] and Ludwieg [4] examined the fully developed laminar boundary layers in rotating curved channel with rectangular and square cross-section, respectively. Their results are valid for the large rotational Reynolds number based on the angular velocity of the channel, as compared with the Reynolds number based on the mean axial velocity of the fluid. Miyazaki [5, 6] analysed the fully developed laminar flow and heat transfer in curved circular/rectangular channels with weak rotations by finite-difference method. Because of the convergence difficulties of the iterative solution method used, Miyazaki's works did not cover the flow range where three forces (centrifugal, Coriolis and centrifugal-type buoyancy forces) are of comparable magnitude. In addition, all the works employ a steady model for the fully developed laminar flows with a positive rotation of the channel. Hereinafter, *positive rotation* means the rotation in the same direction as the axial flow imposed by a pressure gradient, and *negative rotation* means the rotation opposing the flow due to the pressure gradient.

As the existing solutions to the problem are constrained to the asymptotic limits of slow and rapid rotation, the secondary flow revealed by the works mentioned above consists of one-pair of counter-rotating vortices. The interaction of the secondary flow with the pressure-driven main flow causes a shift in the location of the maximum axial velocity away from the centre of the channel and in the direction of the

† Present address: School of Mechanical and Production Engineering, Nanyang Technological University, Nanyang Avenue, Singapore 639798.

NOMENCLATURE

a	radius of tube
c	pseudo Reynolds number, equation (5)
c_1	axial pressure gradient, $-(1/R_c)(\partial P'/\partial\theta)$
c_2	axial temperature gradient, $-(1/R_c)(\partial t/\partial\theta)$
c_p	specific heat
c_i^l, c_i^h	constants
De	Dean number
$\hat{De}$	modified Dean number through equation (87)
D_Ω	dynamical parameter defined by equation (82)
$\hat{D}_\Omega$	modified D_Ω through equation (87)
D_r	dynamical parameter defined by equation (82)
$\hat{D}_r$	modified D_r through equation (87)
f	mean friction factor
f_s	mean friction factor for a stationary straight tube
h	heat transfer coefficent
L_1	parameter defined by equation (42)
L_2	parameter defined by equation (42)
Nu	mean Nusselt number
Nu_s	mean Nusselt number for a stationary straight tube
r, R	coordinates
Ra_Ω	rotational Rayleigh number, equation (5)
R_c	curvature radius
Re	Reynolds number, equation (74)
$\hat{Re}$	modified Reynolds number through equation (87)
Re_Ω	rotational Reynolds number, equation (5)
$o'z'$	axis of curvature and rotation
p	fluid pressure
p'	pseudo pressure, $P' = p - \rho_w\Omega^2(R_c + R\sin\varphi)^2/2$
Pr	Prandtl number, equation (5)
q_w	wall heat flux
Q	flow rate
Q_1	defined by equation (72)
Q_s	flow rate through a stationary straight tube
t	temperature of fluid
t_m	mean temperature of fluid
t_w	wall temperature
U, V, W	velocity components
w	nondimensional main velocity, equation (4)
w_m	mean main velocity
w_{ijk}	expansion coefficient for w
w_{ijk}^{lm}	parameter free expansion coefficients for w
x_i	variable.

Greek symbols

α	thermal diffusivity
β	coefficient of thermal expansion
η	nondimensional temperature
η_c	extreme value of η
η_m	mean temperature across the tube
η_{ijk}	expansion coefficient for η
η_{ijk}^{lm}	parameter free expansion coefficients for η
Γ	defined by equation (81)
λ	conductivity of fluid
ν	kinematic viscosity
Ω	angular velocity
ϕ	nondimensional stream function, equation (4)
ϕ_{ijk}	expansion coefficient for ϕ
ϕ_{ijk}^{lm}	parameter free expansion coefficients for ϕ
ρ	density of fluid
ρ_w	density of fluid based on wall temperature
σ	curvature ratio, equation (5)
θ	polar coordinate
ε_1, ε_2, ε_3	σ, Re_Ω, Ra_Ω
φ	coordinate.

secondary velocities in the middle of the channel. When the three forces are of comparable magnitude, however, a complicated structure of the secondary flow might be expected since then the nonlinear effects could be quite strong.

In the present work, a three-parameter, regular perturbation method is developed to study laminar flow transitions and combined free and forced convective heat transfer in a rotating curved circular tube. The specific problem considered is the curved tube rotating at a constant angular velocity about the axis through the centre of the curvature. A full second-order perturbation solution is obtained for the full nonlinear coupled governing equations under the conditions that the flow and temperature fields are fully developed, and the wall heat flux is uniform with peripherally uniform wall temperature. The solution covers both heating and cooling cases, with either positive or negative rotation. By excluding the effect of any one or two of the three factors (rotation, cur-

vature and heating/cooling), the solution reduces to each of the six special problems such as the classical Dean problem and mixed convection problem.

2. FORMULATION AND PERTURBATION SOLUTION

The geometrical configuration of the physical model for a rotating curved circular tube and its coordinate system are shown in Fig. 1. Under the action of the pressure gradient, a viscous fluid is allowed through the curved tube of circular cross-section of radius a with negligible pitch effect, which is rotated about the axis through the centre of the curvature $o'z'$ with a constant angular velocity Ω. The tube is being uniformly heated or cooled at the wall with a heat flux q_w. The properties of the fluid, with the exception of density, are taken to be constant.

Consider a toroidal coordinate system (R, φ, θ) fixed to the rotating curved tube as shown in Fig. 1. The direction of the main flow in the tube is chosen in the direction of increasing θ, while the angular velocity of the tube is taken as $\Omega > 0$ for increasing θ and $\Omega < 0$ for decreasing θ, respectively. The velocity components in the increasing directions of R, φ, and θ are denoted by U, V, W, respectively. The buoyancy term is expressed in terms of the coefficient of thermal expansion as is commonly done in free-convection analyses (Boussinesq approximation). The temperature difference used to express density variations in the buoyancy term is $t_w - t$. In the case of hydrodynamically and thermally fully developed laminar flow under the condition that the wall heat flux is uniform with peripherally uniform wall temperature, the governing equations are given, in terms of the dimensionless variables and the secondary flow stream function, as [7]

$$D^4\phi = \frac{1}{r(1+\sigma r\sin\varphi)}\frac{\partial(\phi, D^2\phi)}{\partial(r,\varphi)} - \frac{2\sigma}{(1+\sigma r\sin\varphi)^2}\frac{\partial\phi}{\partial y}D^2\phi - \left[2\sigma w + \frac{Re_\Omega}{2}(1+\sigma r\sin\varphi)\right]\frac{\partial w}{\partial y} - Ra_\Omega(1+\sigma r\sin\varphi)^2\frac{\partial\eta}{\partial y} \quad (1)$$

$$\nabla^2 w = \frac{1}{1+\sigma r\sin\varphi}\left[\frac{1}{r}\frac{\partial(\phi, w)}{\partial(r,\varphi)} - \sigma\frac{\partial w}{\partial x} + \frac{Re_\Omega}{2}\frac{\partial\phi}{\partial y} - 4c\right] + \frac{\sigma w}{(1+\sigma r\sin\varphi)^2}\left(\frac{\partial\phi}{\partial y} + \sigma\right) \quad (2)$$

$$\nabla^2\eta = \frac{1}{1+\sigma r\sin\varphi}\left[\frac{Pr}{r}\frac{\partial(\phi,\eta)}{\partial(r,\varphi)} + w - \sigma\frac{\partial\eta}{\partial x}\right] \quad (3)$$

in which

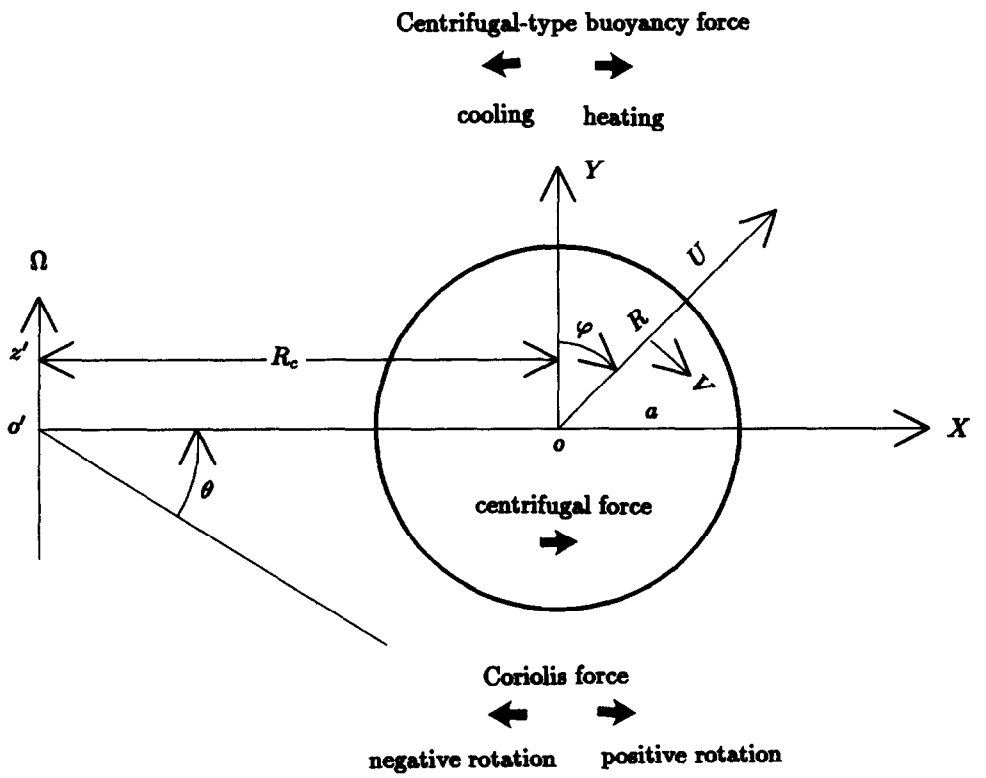

Fig. 1. Geometrical configuration and coordinate system.

$$\frac{\partial}{\partial x} = \sin\varphi \frac{\partial}{\partial r} + \frac{\cos\varphi}{r} \frac{\partial}{\partial \varphi};$$

$$\frac{\partial}{\partial y} = \cos\varphi \frac{\partial}{\partial r} - \frac{\sin\varphi}{r} \frac{\partial}{\partial \varphi}$$

$$D^2 = \nabla^2 - \frac{\sigma}{1+\sigma r \sin\varphi} \frac{\partial}{\partial x};$$

$$\nabla^2 = \frac{\partial^2}{\partial r^2} + \frac{1}{r}\frac{\partial}{\partial r} + \frac{1}{r^2}\frac{\partial^2}{\partial \varphi^2}.$$

The dimensionless variables are defined as

$$r = \frac{R}{a}; \quad U = -\frac{\nu R_c}{R(R_c + R\sin\varphi)} \frac{\partial \phi}{\partial \varphi};$$

$$V = \frac{\nu R_c}{R_c + R\sin\varphi} \frac{\partial \phi}{\partial R}; \quad w = \frac{Wa}{\nu}; \quad \eta = \frac{t_w - t}{Pr c_2 a} \tag{4}$$

and the dimensionless parameters are defined as

$$\sigma = \frac{a}{R_c}; \quad Pr = \frac{\nu}{\alpha}; \quad c = \frac{c_1 a^3}{4\rho\nu^2};$$

$$Re_\Omega = \frac{4\Omega a^2}{\nu}; \quad Ra_\Omega = \frac{Pr\beta\Omega^2 c_2 a^4 R_c}{\nu^2}. \tag{5}$$

We seek the solution of equations (1)–(3) subject to the condition of no-slip at the wall and the uniform wall heat flux with peripherally uniform wall temperature, namely,

$$\frac{\partial \phi}{\partial r} = \frac{\partial \phi}{\partial \varphi} = w = \eta = 0 \quad \text{at } r = 1. \tag{6}$$

Further in the region $0 \leqslant r \leqslant 1$ and $-\pi \leqslant \varphi \leqslant \pi$

$$\frac{\partial \phi}{\partial r}, \quad \frac{\partial \phi}{\partial \varphi}, \quad w, \quad \text{and} \quad \eta \text{ must be finite.} \tag{7}$$

The solutions of equations (1)–(3) under the boundary conditions (6) and (7) are governed by five dimensionless parameters: σ, Pr, c, Re_Ω and Ra_Ω. The curvature ratio σ, a geometry parameter, represents the degree of curvature. Prandtl number Pr, a thermophysical property parameter, represents the ratio of momentum diffusion rate to that of thermal diffusion. c is defined in an identical mathematical form to the usual Reynolds number Re, but using pseudo pressure instead of the usual fluid pressure. It represents the ratio of inertial force to viscous force. The rotational Reynolds number Re_Ω emerges from the Coriolis term of the momentum equations. It represents the ratio of the Coriolis force to the viscous force. A positive Re_Ω represents the case of positive rotation. A negative Re_Ω is for the case of negative rotation. The rotational Rayleigh number Ra_Ω has its origin in the centrifugal buoyancy terms. It is similar to the Rayleigh number encountered in the study of gravitational buoyancy due to the Earth's gravitational field, but with the gravitational acceleration replaced by the centrifugal acceleration measured at the centreline of the tube considered. It denotes the ratio of centrifugal-type buoyancy force to the viscous force. A positive Ra_Ω represents the cooling case, while a negative Ra_Ω is for the case of heating.

Although an exact solution of equations (1)–(3) would be extremely difficult to find, if indeed possible, an approximate solution may readily be obtained using a parameter perturbation method with power sequence as the expansion functions. A theoretical basis for this method can be found in ref. [7], which shows that any function of m variables $x_1, x_2, \ldots, x_m$ which is continuous for $c_i^l \leqslant x_i \leqslant c_i^h$ $(i = 1, 2, \ldots, m)$ may be approximated uniformly by a unique polynomial. The reason to choose the power sequence as the expansion functions is because of the uniqueness of the expansion and its uniform convergence rather than just convergence in the mean. In the literature, the perturbation solution is usually considered to be valid only for small values of perturbation parameters. However, we can always, in principle, find a proper mathematical transformation to make the perturbation parameter small enough so that the solution is valid. The theoretical basis shown in ref. [7] also shows that we can achieve any accuracy required by a suitable choice of the number of terms in the perturbation series for the entire region of the parameters. And the high order terms can be obtained through a computer [8, 9]. The main drawback of the perturbation method with the power sequence as the expansion functions is that it cannot be used to obtain a discontinuous solution which usually exists in the nonlinear problems. This leads to a disagreement between the perturbation solution and the numerical solution for Dean problem and mixed convection problem [10, 11] by noting that the numerical solution is a discontinuous one due to the bifurcation of the flow at intermediate and large values of the corresponding dynamical parameters.

Applying to the present problem, the method involves the expansion of the stream function ϕ, nondimensional main velocity w and temperature η in ascending powers of the suitable small parameters. σ, Re_Ω and Ra_Ω are selected as the parameters in this work. This implies the assumption of continuity of ϕ, w and η on σ, Re_Ω and Ra_Ω. Then each of the coefficients of the expansion series for ϕ, w and η may be obtained from the solutions of the associated nonhomogeneous harmonic and biharmonic differential equations. In calculating each additional term of the series, the terms on the right hand sides of the harmonic and biharmonic differential equations, are in terms of the functions determined from the solution of the preceding equations. Therefore successive solutions of the three main differential equations will produce as many terms as desired for the three series depending upon the accuracy required. In this work, the solution is carried up to and including the second-order terms.

Let

$$\left.\begin{aligned}\phi &= \sum_{i=0}^{\infty}\sum_{j=0}^{\infty}\sum_{k=0}^{\infty}\phi_{ijk}\varepsilon_1^i\varepsilon_2^j\varepsilon_3^k\\ w &= \sum_{i=0}^{\infty}\sum_{j=0}^{\infty}\sum_{k=0}^{\infty}w_{ijk}\varepsilon_1^i\varepsilon_2^j\varepsilon_3^k\\ \eta &= \sum_{i=0}^{\infty}\sum_{j=0}^{\infty}\sum_{k=0}^{\infty}\eta_{ijk}\varepsilon_1^i\varepsilon_2^j\varepsilon_3^k\end{aligned}\right\}, \tag{8}$$

where ε_1, ε_2 and ε_3 denote, respectively, σ, Re_Ω and Ra_Ω, and the coefficients depend on the coordinates of the points of the fluid (r, φ).

On substitution of equation (8) into equations (1)–(3), sets of equations for the zeroth, first- and second-order coefficients may be obtained by equating the coefficients of equal powers of $\varepsilon_1^i\varepsilon_2^j\varepsilon_3^k$. Since there can be no flow in the (r, φ)-plane when $\sigma = Re_\Omega = Ra_\Omega = 0$, it follows that $\phi_{000} = 0$. The resulting equations for the coefficients up to and including second-order are as follows:

zeroth-order

$$\nabla^2 w_{000} = -4c \tag{9}$$

$$\nabla^2 \eta_{000} = w_{000} \tag{10}$$

first-order

$$\nabla^4 \phi_{100} = -2w_{000}\frac{\partial w_{000}}{\partial y} \tag{11}$$

$$\nabla^4 \phi_{010} = \frac{1}{2}\frac{\partial w_{000}}{\partial y} \tag{12}$$

$$\nabla^4 \phi_{001} = -\frac{\partial \eta_{000}}{\partial y} \tag{13}$$

$$\nabla^2 w_{100} = \frac{1}{r}\frac{\partial(\phi_{100}, w_{000})}{\partial(r,\varphi)} - \frac{\partial w_{000}}{\partial y} + 4cr\sin\varphi \tag{14}$$

$$\nabla^2 w_{010} = \frac{1}{r}\frac{\partial(\phi_{010}, w_{000})}{\partial(r,\varphi)} \tag{15}$$

$$\nabla^2 w_{001} = \frac{1}{r}\frac{\partial(\phi_{001}, w_{000})}{\partial(r,\varphi)} \tag{16}$$

$$\nabla^2 \eta_{100} = \frac{Pr}{r}\frac{\partial(\phi_{100}, \eta_{000})}{\partial(r,\varphi)} + w_{100} - \frac{\partial \eta_{000}}{\partial x} - rw_{000}\sin\varphi \tag{17}$$

$$\nabla^2 \eta_{010} = \frac{Pr}{r}\frac{\partial(\phi_{010}, \eta_{000})}{\partial(r,\varphi)} + w_{010} \tag{18}$$

$$\nabla^2 \eta_{001} = \frac{Pr}{r}\frac{\partial(\phi_{001}, \eta_{000})}{\partial(r,\varphi)} + w_{001} \tag{19}$$

second-order

$$\nabla^2 \phi_{200} = \frac{1}{r}\frac{\partial(\phi_{100}, \nabla^2\phi_{100})}{\partial(r,\varphi)} + 2\frac{\partial \nabla^2 \phi_{100}}{\partial x} - 2w_{000}\frac{\partial w_{100}}{\partial y} - 2w_{100}\frac{\partial w_{000}}{\partial y} \tag{20}$$

$$\nabla^2 \phi_{020} = \frac{1}{r}\frac{\partial(\phi_{010}, \nabla^2\phi_{010})}{\partial(r,\varphi)} - \frac{1}{2}\frac{\partial w_{010}}{\partial y} \tag{21}$$

$$\nabla^2 \phi_{002} = \frac{1}{r}\frac{\partial(\phi_{001}, \nabla^2\phi_{001})}{\partial(r,\varphi)} - \frac{\partial \eta_{010}}{\partial y} \tag{22}$$

$$\nabla^4 \phi_{110} = \frac{1}{r}\frac{\partial(\phi_{100}, \nabla^2\phi_{100})}{\partial(r,\varphi)} + \frac{1}{r}\frac{\partial(\phi_{010}, \nabla^2\phi_{100})}{\partial(r,\varphi)} + 2\frac{\partial \nabla^2 \phi_{010}}{\partial x} - 2w_{000}\frac{\partial w_{010}}{\partial y} - 2w_{010}\frac{\partial w_{000}}{\partial y} - \frac{1}{2}\frac{\partial w_{100}}{\partial y} - \frac{1}{2}r\sin\varphi\frac{\partial w_{000}}{\partial y} \tag{23}$$

$$\nabla^4 \phi_{101} = \frac{1}{r}\frac{\partial(\phi_{100}, \nabla^2\phi_{001})}{\partial(r,\varphi)} + \frac{1}{r}\frac{\partial(\phi_{001}, \nabla^2\phi_{100})}{\partial(r,\varphi)} + 2\frac{\partial \nabla^2 \phi_{001}}{\partial x} - 2w_{000}\frac{\partial w_{001}}{\partial y} - 2w_{001}\frac{\partial w_{000}}{\partial y} - \frac{\partial \eta_{100}}{\partial y} - 2r\sin\varphi\frac{\partial \eta_{000}}{\partial y} \tag{24}$$

$$\nabla^4 \phi_{011} = \frac{1}{r}\frac{\partial(\phi_{010}, \nabla^2\phi_{001})}{\partial(r,\varphi)} + \frac{1}{r}\frac{\partial(\phi_{001}, \nabla^2\phi_{010})}{\partial(r,\varphi)} - \frac{1}{2}\frac{\partial w_{001}}{\partial y} - \frac{\partial \eta_{010}}{\partial y} \tag{25}$$

$$\nabla^2 w_{200} = \frac{1}{r}\frac{\partial(\phi_{200}, w_{000})}{\partial(r,\varphi)} + \frac{1}{r}\frac{\partial(\phi_{100}, w_{100})}{\partial(r,\varphi)} - \sin\varphi\frac{\partial(\phi_{100}, w_{000})}{\partial(r,\varphi)} + r\sin\varphi\frac{\partial w_{000}}{\partial x} - \frac{\partial w_{100}}{\partial x} + w_{000} + w_{000}\frac{\partial \phi_{100}}{\partial y} - 4cr^2\sin^2\varphi. \tag{26}$$

$$\nabla^2 w_{020} = \frac{1}{r}\frac{\partial(\phi_{020}, w_{000})}{\partial(r,\varphi)} + \frac{1}{r}\frac{\partial(\phi_{010}, w_{010})}{\partial(r,\varphi)} + \frac{1}{2}\frac{\partial \phi_{010}}{\partial y} \tag{27}$$

$$\nabla^2 w_{002} = \frac{1}{r}\frac{\partial(\phi_{002}, w_{000})}{\partial(r,\varphi)} + \frac{1}{r}\frac{\partial(\phi_{001}, w_{001})}{\partial(r,\varphi)} \tag{28}$$

$$\nabla^2 w_{110} = \frac{1}{r}\frac{\partial(\phi_{110}, w_{000})}{\partial(r,\varphi)} + \frac{1}{r}\frac{\partial(\phi_{100}, w_{010})}{\partial(r,\varphi)} + \frac{1}{r}\frac{\partial(\phi_{010}, w_{100})}{\partial(r,\varphi)} - \sin\varphi\frac{\partial(\phi_{010}, w_{000})}{\partial(r,\varphi)} - \frac{\partial w_{010}}{\partial x} + \frac{1}{2}\frac{\partial \phi_{100}}{\partial y} + w_{000}\frac{\partial \phi_{010}}{\partial y} \tag{29}$$

$$\nabla^2 w_{101} = \frac{1}{r}\frac{\partial(\phi_{101}, w_{000})}{\partial(r,\varphi)} + \frac{1}{r}\frac{\partial(\phi_{100}, w_{001})}{\partial(r,\varphi)} + \frac{1}{r}\frac{\partial(\phi_{001}, w_{100})}{\partial(r,\varphi)} - \sin\varphi\frac{\partial(\phi_{001}, w_{000})}{\partial(r,\varphi)} - \frac{\partial w_{001}}{\partial x} + w_{000}\frac{\partial\phi_{001}}{\partial y} \quad (30)$$

$$\nabla^2 w_{011} = \frac{1}{r}\frac{\partial(\phi_{011}, w_{000})}{\partial(r,\varphi)} + \frac{1}{r}\frac{\partial(\phi_{010}, w_{001})}{\partial(r,\varphi)} + \frac{1}{r}\frac{\partial(\phi_{001}, w_{010})}{\partial(r,\varphi)} + \frac{1}{2}\frac{\partial\phi_{001}}{\partial y} \quad (31)$$

$$\nabla^2\eta_{200} = \frac{Pr}{r}\frac{\partial(\phi_{200}, \eta_{000})}{\partial(r,\varphi)} + \frac{Pr}{r}\frac{\partial(\phi_{100}, \eta_{100})}{\partial(r,\varphi)} + w_{200} + \frac{\partial\eta_{100}}{\partial x} + r\sin\varphi\nabla^2\eta_{100} \quad (32)$$

$$\nabla^2\eta_{020} = \frac{Pr}{r}\frac{\partial(\phi_{020}, \eta_{000})}{\partial(r,\varphi)} + \frac{Pr}{r}\frac{\partial(\phi_{010}, \eta_{010})}{\partial(r,\varphi)} + w_{020} \quad (33)$$

$$\nabla^2\eta_{002} = \frac{Pr}{r}\frac{\partial(\phi_{020}, \eta_{000})}{\partial(r,\varphi)} + \frac{Pr}{r}\frac{\partial(\phi_{001}, \eta_{001})}{\partial(r,\varphi)} + w_{002} \quad (34)$$

$$\nabla^2\eta_{110} = \frac{Pr}{r}\frac{\partial(\phi_{110}, \eta_{000})}{\partial(r,\varphi)} + \frac{Pr}{r}\frac{\partial(\phi_{100}, \eta_{010})}{\partial(r,\varphi)} + \frac{Pr}{r}\frac{\partial(\phi_{010}, \eta_{100})}{\partial(r,\varphi)} + w_{110} - \frac{\partial\eta_{010}}{\partial x} - r\sin\varphi\nabla^2\eta_{010} \quad (35)$$

$$\nabla^2\eta_{101} = \frac{Pr}{r}\frac{\partial(\phi_{101}, \eta_{000})}{\partial(r,\varphi)} + \frac{Pr}{r}\frac{\partial(\phi_{100}, \eta_{001})}{\partial(r,\varphi)} + \frac{Pr}{r}\frac{\partial(\phi_{001}, \eta_{100})}{\partial(r,\varphi)} + w_{101} - \frac{\partial\eta_{001}}{\partial x} - r\sin\varphi\nabla^2\eta_{001} \quad (36)$$

$$\nabla^2\eta_{011} = \frac{Pr}{r}\frac{\partial(\phi_{011}, \eta_{000})}{\partial(r,\varphi)} + \frac{Pr}{r}\frac{\partial(\phi_{010}, \eta_{001})}{\partial(r,\varphi)} + \frac{Pr}{r}\frac{\partial(\phi_{001}, \eta_{010})}{\partial(r,\varphi)} + w_{011}. \quad (37)$$

Similarly, we may obtain equations corresponding to the third and higher approximations.

Solving equations (9)–(37) in order yields:

stream function of secondary flow

$$\phi_{100} = \frac{c^2}{288}r(1-r^2)^2(4-r^2)\cos\varphi \quad (38)$$

$$\phi_{010} = \frac{c}{192}r(1-r^2)^2\cos\varphi \quad (39)$$

$$\phi_{001} = \frac{c}{4608}r(1-r^2)^2(r^2-10)\cos\varphi \quad (40)$$

$$\phi_1 = \sigma\phi_{100} + Re_\Omega\phi_{010} + Ra_\Omega\phi_{001} = \frac{\sigma c^2}{288}r(1-r^2)^2[4-r^2+L_2(r^2-10)+L_1]\cos\varphi, \quad (41)$$

where

$$L_1 = \frac{3Re_\Omega}{2\sigma c}, \quad L_2 = \frac{Ra_\Omega}{16\sigma c} \quad (42)$$

$$\phi_{200} = \frac{c^4\sin 2\varphi}{350\times 1152^2}r^2(1-r^2)^2(4979-2792r^2+779r^4-134r^6+5r^8) - \frac{c^4\sin 2\varphi}{5760}r^2(1-r^2)^2(16-7r^2) \quad (43)$$

$$\phi_{020} = \frac{c^2\sin 2\varphi}{30\times 768^2}r^2(1-r^2)^2(17-2r^2-r^4) \quad (44)$$

$$\phi_{002} = \frac{Prc^2\sin 2\varphi}{44\,800\times 1152^2}(10\,518r^2-25\,260r^4+21\,000r^6-7280r^8+1575r^{10}-168r^{12}+5r^{14}) + \frac{c^2\sin 2\varphi}{89\,600\times 1152^2}(6743r^2-11\,576r^4+840r^6+6160r^8-2380r^{10}+192r^{12}-9r^{14}) \quad (45)$$

$$\phi_{110} = \frac{c^3\sin 2\varphi}{350\times 1152^2}r^2(1-r^2)^2(3111-1228r^2+208r^4-36r^6) + \frac{c\sin 2\varphi}{1024}r^2(1-r^2)^2 \quad (46)$$

$$\phi_{101} = \frac{Prc^3\sin 2\varphi}{2800\times 1152^2}(-4086r^2+10\,050r^4-8400r^6+3080r^8-735r^{10}+96r^{12}-5r^{14}) + \frac{c^3\sin 2\varphi}{2800\times 1152^2}(-7739r^2+18\,608r^4-14\,490r^6+4200r^8-665r^{10}+84r^{12}+2r^{14}) + \frac{c\sin 2\varphi}{20\times 32^2}(-37r^2+78r^4-45r^6+4r^8) \quad (47)$$

$$\phi_{011} = \frac{Prc^2\sin 2\varphi}{537\,600\times 1152^2}(-268r^2+650r^4-525r^6+175r^8-35r^{10}+3r^{12}) + \frac{c^2\sin 2\varphi}{5600\times 1152^2}(-3957r^2+8000r^4-3675r^6-840r^8+490r^{10}-18r^{12}) \quad (48)$$

main velocity

$$w_{000} = c(1-r^2) \quad (49)$$

$$w_{100} = \frac{c^3}{11\,520}r(1-r^2)(19-21r^2+9r^4-r^6)\sin\varphi$$

$$-\frac{3c}{4}r(1-r^2)\sin\varphi \quad (50)$$

$$w_{010}=\frac{c^2 r}{4608}r(1-r^2)(3-3r^2+r^4)\sin\varphi \quad (51)$$

$$w_{001}=\frac{c^2}{160\times 1152}r(r^2-1)(49-51r^2+19r^4-r^6)\sin\varphi \quad (52)$$

$$w_{200}=f_{200}+g_{200}\cos 2\varphi \quad (53)$$

where

$$f_{200}=-\frac{c^5}{2800\times 1152^2}(1-r^2)^4(4119-4804r^2+2410r^4-500r^6+35r^8)-\frac{c^3}{230\,400}(1-r^2)(148+43r^2-132r^4+68r^6-7r^8)-\frac{c}{32}(1-r^2)(3-11r^2)$$

$$g_{200}=-\frac{c^5}{88\,200\times 1152^2}r^2(1-r^2)(145\,690-240\,206r^2+174\,649r^4-70\,547r^6+19\,123r^8-2801r^{10}+160r^{12})+\frac{c^3}{276\,480}r^2(1-r^2)(463-613r^2+296r^4-40r^6)-\frac{5c}{16}r^2(1-r^2)$$

$$w_{020}=f_{020}+g_{020}\cos 2\varphi, \quad (54)$$

where

$$f_{020}=-\frac{c^3}{360\times 768^2}(1-r^2)^4(37-32r^2+10r^4)-\frac{c}{4608}(1-r^2)^3$$

$$g_{020}=-\frac{c^3}{12\,600\times 768^2}r^2(1-r^2)(923-1457r^2+958r^4-302r^6+48r^8)+\frac{c}{18\,432}r^2(1-r^2)(5-3r^2)$$

$$w_{002}=f_{002}+g_{002}\cos 2\varphi \quad (55)$$

with

$$f_{002}=\frac{c^3}{430\,080\times 1152^2}(-16\,525+82\,320r^2-170\,436r^4+189\,728r^6-122\,598r^8+46\,032r^{10}-9268r^{12}+768r^{14}-21r^{16})$$

$$g_{002}=\frac{Prc^3}{9800\times 1152^3}(-362\,375r^2+883\,512r^4-807\,975r^6+352\,800r^8-76\,440r^{10}+11\,340r^{12}-882r^{14}+20r^{16})+\frac{c^3}{1400\times 1152^3}(7325r^2-6090r^4-17\,640r^6+30\,366r^8-17\,850r^{10}+4194r^{12}-315r^{14}+10r^{16})+\frac{c^2}{7\,526\,400\times 1152^2}(-88\,447r^2+188\,804r^4-121\,233r^6+4704r^8+21\,560r^{10}-5712r^{12}+336r^{14}-12r^{16})$$

$$w_{110}=f_{110}+g_{110}\cos 2\varphi \quad (56)$$

with

$$f_{110}=-\frac{c^4}{8400\times 1152^2}(1-r^2)^4(9797-9952r^2+4100r^4-480r^6)-\frac{c^2}{73\,728}(1-r^2)(59-81r^2+39r^4-r^6)$$

$$g_{110}=-\frac{c^4}{5600\times 1152^2}r^2(1-r^2)(6017-9735r^2+6775r^4-2465r^6+545r^8-47r^{10})+\frac{c^2}{92\,160}r^2(1-r^2)(101-89r^2+21r^4)$$

$$w_{101}=f_{101}+g_{101}\cos 2\varphi. \quad (57)$$

Here

$$f_{101}=\frac{c^4}{67\,200\times 1152^2}(31\,951-162\,120r^2+344\,400r^4-397\,880r^6+271\,740r^8-111\,216r^{10}+25\,900r^{12}-2880r^{14}+105r^{16})+\frac{c^2}{6400\times 1152}(771-510r^2-950r^4+1000r^6-325r^8+14r^{10})$$

$$g_{101}=\frac{Prc^4}{705\,600\times 1152^2}(140\,237r^2-343\,224r^4+316\,575r^6-141\,120r^8+32\,340r^{10}-5292r^{12}+540r^{14}-20r^{16})+\frac{c^4}{470\,400\times 1152^2}(146\,801r^2-394\,184r^4+433\,398r^6-263\,424r^8+97\,510r^{10}-22\,512r^{12}+2499r^{14}-88r^{16})+\frac{c^2}{3840\times 1152}(253r^2-644r^4+561r^6-180r^8+10r^{10})$$

$$w_{011}=f_{011}+g_{011}\cos 2\varphi \quad (58)$$

here

$$f_{011} = \frac{c^3}{8400\times 4608^2}(25\,337 - 124\,740r^2 + 253\,890r^4 - 275\,380r^6 + 170\,625r^8 - 59\,472r^{10} + 10\,220r^{12} - 480r^{14}) + \frac{c}{32\times 4608}(13 - 40r^2 + 42r^4 - 16r^6 + r^8)$$

$$g_{011} = \frac{Prc^3}{22\,400\times 1152^2}(1763r^2 - 4288r^4 + 3900r^6 - 1680r^8 + 350r^{10} - 48r^{12} + 3r^{14}) + \frac{c^3}{89\,600\times 1152^2}(7615r^2 - 20\,264r^4 + 21\,810r^6 - 12\,600r^8 + 4130r^{10} - 720r^{12} + 29r^{14}) + \frac{c}{160\times 1152}(-21r^2 + 35r^4 - 15r^6 + r^8)$$

temperature

$$\eta_{000} = -\frac{c}{16}(3 - 4r^2 + r^4) \tag{59}$$

$$\eta_{100} = \frac{Prc^3\sin\varphi}{240\times 1152}(-103r + 240r^3 - 220r^5 + 105r^7 - 24r^9 + 2r^{11}) + \frac{c^3\sin\varphi}{1200\times 1152}(-146r + 285r^3 - 200r^5 + 75r^7 - 15r^9 + r^{11}) + \frac{c\sin\varphi}{96}(19r - 27r^3 + 8r^5) \tag{60}$$

$$\eta_{010} = \frac{Prc^2\sin\varphi}{160\times 1152}(-27r + 60r^3 - 50r^5 + 20r^7 - 3r^9) + \frac{c^2\sin\varphi}{960\times 1152}(-47r + 90r^3 - 60r^5 + 20r^7 - 3r^9) \tag{61}$$

$$\eta_{001} = \frac{Prc^2\sin\varphi}{3840\times 1152}(265r - 600r^3 + 520r^5 - 225r^7 + 42r^9 - 2r^{11}) + \frac{c^2\sin\varphi}{19\,200\times 1152}(381r - 735r^3 + 500r^5 - 175r^7 + 30r^9 - r^{11}) \tag{62}$$

$$\eta_{200} = h_{200} + m_{200}\cos 2\varphi, \tag{63}$$

where

$$h_{200} = \frac{Pr^2c^5}{302\,400\times 1152^2}(97\,207 - 519\,120r^2 + 1\,188\,810r^4 - 1\,536\,360r^6 + 1\,242\,045r^8 - 655\,452r^{10} + 225\,540r^{12} - 48\,060r^{14} + 5670r^{16} - 280r^{18}) + \frac{Prc^5}{525\times 1152^3}(58\,721 - 294\,336r^2 + 618\,408r^4 - 712\,488r^6 + 498\,456r^8 - 223\,776r^{10} + 66\,276r^{12} - 12\,528r^{14} + 1323r^{16} - 56r^{18}) + \frac{c^5}{2800\times 11\,340\times 1152^2}(4\,741\,147 - 11\,677\,365r^2 + 15\,082\,200r^4 - 14\,597\,100r^6 + 9\,823\,275r^8 - 4\,516\,722r^{10} + 1\,384\,740r^{12} - 267\,300r^{14} + 28\,350r^{16} - 1225r^{18}) + \frac{Prc^3}{50\times 1152^2}(-7877 + 51\,780r^2 - 105\,300r^4 + 99\,800r^6 - 48\,975r^8 + 11\,592r^{10} - 1020r^{12}) + \frac{c^3}{19\,200\times 1152}(2905 - 2968r^2 - 1080r^4 + 1800r^6 - 825r^8 + 180r^{10} - 12r^{12}) + \frac{c}{384}(-6 - 28r^2 + 51r^4 - 17r^6)$$

$$m_{200} = \frac{Pr^2c^5}{100\,800\times 1152^2}(-2132r^2 - 4620r^4 + 27\,510r^6 - 41\,748r^8 + 31\,395r^{10} - 13\,176r^{12} + 3150r^{14} - 400r^{16} + 21r^{18}) + \frac{Prc^5}{1750\times 1152^3}(806\,072r^2 - 2\,292\,480r^4 + 2\,711\,190r^6 - 1\,762\,464r^8 + 680\,400r^{10} - 167\,760r^{12} + 27\,595r^{14} - 2640r^{16} + 87r^{18}) + \frac{c^5}{3675\times 1152^3}(239\,005r^2 - 582\,760r^4 + 578\,844r^6 - 331\,884r^8 + 122\,598r^{10} - 30\,744r^{12} + 5481r^{14} - 564r^{16} + 24r^{18}) + \frac{Prc^3}{67\,200\times 1152}(-12\,189r^2 + 31\,220r^4 - 32\,340r^6 + 17\,458r^8 - 4585r^{10} + 436r^{12}) + \frac{c^3}{175\times 1152^2}(-24\,034r^2 + 52\,360r^4 - 42\,945r^6 + 18\,396r^8 - 4095r^{10} + 318r^{12}) + \frac{c}{1536}(149r^2 - 220r^4 + 71r^6)$$

$$\eta_{020} = h_{020} + m_{020}\cos 2\varphi \tag{64}$$

here

$$h_{020} = \frac{Pr^2c^3}{11\,200\times 1152^2}(563 - 2835r^2 + 5985r^4 - 6895r^6 + 4725r^8 - 1953r^{10} + 455r^{12} - 45r^{14}) + \frac{Prc^3}{134\,400\times 1152^2}(2071 - 9870r^2 + 19\,320r^4 - 20\,090r^6 + 12\,075r^8 - 4326r^{10} + 910r^{12} - 90r^{14}) + \frac{c^3}{125\,440\times 1152^2}(3029 - 7252r^2 + 8820r^4 - 7840r^6 + 4655r^8 - 1764r^{10} + 392r^{12} - 40r^{14})$$

$$+\frac{c}{768\times1152}(25-48r^2+36r^4-16r^6+3r^8)$$

$$m_{020}=\frac{Pr^2c^3}{89\,600\times1152^2}(37r^2-1680r^4+4830r^6$$
$$-5600r^8+3220r^{10}-912r^{12}+105r^{14})$$
$$+\frac{Prc^3}{134\,400\times1152^2}(5245r^2-14\,000r^4+14\,700r^6$$
$$-7644r^8+1855r^{10}-156r^{12})$$
$$+\frac{c^3}{134\,400\times1152^2}(766r^2-1846r^4+1785r^6$$
$$-966r^8+315r^{10}-60r^{12}+6r^{14})$$
$$+\frac{c}{960\times1152}(-13r^2+25r^4-15r^6+3r^8)$$

$$\eta_{002}=h_{002}+m_{002}\cos2\varphi, \tag{65}$$

where

$$h_{002}=\frac{Pr^2c^3}{13\,440\times1152^3}(129\,578-667\,800r^2$$
$$+1\,457\,190r^4-1\,762\,320r^6+1\,300\,005r^8-604\,044r^{10}$$
$$+173\,124r^{12}-27\,756r^{14}+2079r^{16}-56r^{18})$$
$$+\frac{Prc^3}{67\,200\times1152^3}(197\,494-960\,120r^2+1\,934\,226r^4$$
$$-2\,100\,588r^6+1\,351\,413r^8-539\,784r^{10}$$
$$+136\,080r^{12}-20\,016r^{14}+1323r^{16}-28r^{18})$$
$$+\frac{c^3}{6125\times1152^4}(32\,257\,522-78\,080\,625r^2$$
$$+97\,240\,500r^4-89\,478\,900r^6+56\,029\,050r^8$$
$$-23\,171\,022r^{10}+6\,041\,700r^{12}-893\,700r^{14}$$
$$+56\,700r^{16}-1225r^{18})$$

$$m_{002}=\frac{Pr^2c^3}{224\times537\,600\times1152^2}(843\,810r^2-2\,640\,232r^4$$
$$+3\,586\,156r^6-2\,779\,560r^8+1\,308\,790r^{10}$$
$$-375\,984r^{12}+61\,397r^{14}-4496r^{16}+119r^{18})$$
$$+\frac{Prc^3}{960\times9800\times1152^3}(35\,391\,181r^2-89\,303\,680r^4$$
$$+86\,668\,470r^6-39\,870\,432r^8+6\,703\,200r^{10}$$
$$+624\,960r^{12}-223\,020r^{14}+10\,080r^{16}-759r^{18})$$
$$+\frac{c^3}{134\,400\times1152^3}(-32\,212r^2+58\,600r^4-18\,270r^6$$
$$-28\,224r^8+30\,366r^{10}-12\,240r^{12}+2097r^{14}$$
$$-120r^{16}+3r^{18})+\frac{c^2}{1\,568\,000\times1152^3}(795\,951r^2$$
$$-1\,768\,940r^4+1\,416\,030r^6-484\,932r^8+11\,760r^{10}$$
$$+36\,960r^{12}-7140r^{14}+320r^{16}-9r^{18})$$

$$\eta_{110}=h_{110}+m_{110}\cos2\varphi \tag{66}$$

where

$$h_{110}=\frac{Pr^2c^4}{134\,400\times1152^2}(34\,163-177\,240r^2+390\,180r^4$$
$$-477\,400r^6+357\,420r^8-169\,008r^{10}+49\,280r^{12}$$
$$-7920r^{14}+525r^{16})+\frac{Prc^4}{268\,800\times1152^2}(20\,795$$
$$-101\,696r^2+206\,556r^4-226\,912r^6+148\,330r^8$$
$$-60\,480r^{10}+15\,596r^{12}-2336r^{14}+147r^{16})$$
$$+\frac{c^4}{940\,800\times1152^2}(112\,955-274\,316r^2+343\,980r^4$$
$$-319\,480r^6+202\,615r^8-85\,260r^{10}+22\,736r^{12}$$
$$-3440r^{14}+210r^{16})+\frac{Prc^2}{19\,200\times1152}(-1027$$
$$+6510r^2-12\,450^4+10\,600r^6-4275r^8+642r^{10})$$
$$+\frac{c^2}{38\,400\times1152}(5407-8380r^2+3900r^4-1000r^6$$
$$+25r^8+48r^{10})$$

$$m_{110}=\frac{Pr^2c^4}{67\,200\times1152^2}(-508r^2-4340r^4+16\,275r^6$$
$$-21\,392r^8+14\,070r^{10}-4920r^{12}+875r^{14}-60r^{16})$$
$$+\frac{Prc^4}{1225\times1152^3}(364\,057r^2-1\,010\,310r^4+1\,143\,072r^6$$
$$-688\,086r^8+232\,260r^{10}-46\,746r^{12}+6195r^{14}$$
$$-442r^{16})+\frac{c^4}{1225\times1152^3}(52\,085r^2-126\,357r^4$$
$$+124\,047r^6-69\,342r^8+24\,255r^{10}-5418r^{12}+777r^{14}$$
$$-47r^{16})+\frac{Prc^2}{7680\times1152}(-30r^2+40r^4-45r^6$$
$$+56r^8-21r^{10})+\frac{c^2}{1920\times1152}(-136r^2+277r^4$$
$$-195r^6+62r^8-8r^{10})$$

$$\eta_{101}=h_{101}+m_{101}\cos2\varphi \tag{67}$$

here

$$h_{101}=\frac{Pr^2c^4}{4200\times1152^3}(-501\,881+2\,633\,400r^2$$

$$-5\,889\,240r^4+7\,369\,320r^6-5\,700\,870r^8+2\,831\,976r^{10}$$
$$-894\,600r^{12}+167\,400r^{14}-16\,065r^{16}+560r^{18})$$
$$+\frac{Prc^4}{8400\times1152^3}(-304\,597+1\,503\,936r^2-3\,095\,820r^4$$
$$+3\,467\,184r^6-2\,331\,882r^8+991\,872r^{10}-272\,916r^{12}$$
$$+46\,080r^{14}-3969r^{16}+112r^{18})$$
$$+\frac{c^4}{441\,000\times1152^3}(-24\,731\,219$$
$$+60\,387\,390r^2-76\,601\,700r^4$$
$$+72\,324\,000r^6-46\,999\,575r^8+20\,543\,544r^{10}$$
$$-5\,838\,840r^{12}+999\,000r^{14}-85\,050r^{16}+2450r^{18})$$
$$+\frac{Prc^2}{800\times1152^2}(20\,201-129\,900r^2+254\,700r^4$$
$$-227\,000r^6+100\,275r^8-19\,296r^{10}$$
$$+1020r^{12})+\frac{c^2}{307\,200\times1152}(-7623+7728r^2$$
$$+2880r^4-4600r^6+1975r^8-372r^{10}+12r^{12})$$

$$m_{101}=\frac{Pr^2c^4}{19\,600\times1152^3}(-901\,994r^2+3\,239\,712r^4$$
$$-5\,184\,816r^6+4\,770\,192r^8-2\,672\,460r^{10}+913\,248r^{12}$$
$$-181\,167r^{14}+17\,936r^{16}-651r^{18})$$
$$+\frac{Prc^4}{294\,000\times1152^3}(-28\,769\,699r^2+79\,473\,200r^4$$
$$-89\,945\,730r^6+54\,780\,768r^8-19\,051\,200r^{10}$$
$$+4\,049\,640r^{12}-584\,325r^{14}+47\,880r^{16}-534r^{18})$$
$$+\frac{c^4}{49\,000\times1152^3}(-598\,003r^2+1\,468\,010r^4$$
$$-1\,478\,190r^6+866\,796r^8-329\,280r^{10}+83\,580r^{12}$$
$$-14\,070r^{14}+1190r^{16}-33r^{18})$$
$$+\frac{Prc^2}{1\,075\,200\times1152}(-56\,141r^2+146\,580r^4$$
$$-144\,585r^6+66\,262r^8-12\,880r^{10}+764r^{12})$$
$$+\frac{c^2}{2800\times1152^2}(18\,554r^2-33\,740r^4+19\,845r^6$$
$$-5376r^8+735r^{10}-18r^{12})$$

$$\eta_{011}=h_{011}+m_{011}\cos2\varphi, \tag{68}$$

where

$$h_{011}=\frac{Pr^2c^3}{2\,150\,400\times1152^2}(-88\,211+449\,400r^2$$
$$-964\,740r^4+1\,139\,320r^6-811\,020r^8+356\,496r^{10}$$
$$-92\,960r^{12}+12\,240r^{14}-525r^{16})$$
$$+\frac{Prc^3}{4\,300\,800\times1152^2}(-53\,931+259\,616r^2-515\,676r^4$$
$$+548\,352r^6-341\,530r^8+129\,696r^{10}-30\,156r^{12}$$
$$+3776r^{14}-147r^{16})+\frac{c^3}{940\,800\times4608^2}(-294\,695$$
$$+709\,436r^2-873\,180r^4+789\,880r^6-481\,915r^8$$
$$+191\,100r^{10}-46\,256r^{12}+5840r^{14}-210r^{16})$$
$$+\frac{c}{9600\times4608}(-503+975r^2-750r^4$$
$$+350r^6-75r^8+3r^{10})$$

$$m_{011}=\frac{Pr^2c^3}{6\times1120^2\times1152^2}(-130\,520r^2+461\,132r^4$$
$$-711\,921r^6+613\,424r^8-307\,230r^{10}+86\,856r^{12}$$
$$-12\,257r^{14}+516r^{16})+\frac{Prc^3}{140^2\times1152^3}(-540\,835r^2$$
$$+1\,419\,138r^4-1\,458\,072r^6+736\,806r^8-167\,580r^{10}$$
$$+9954r^{12}+567r^{14}+22r^{16})$$
$$+\frac{c^3}{140^2\times1152^3}(-65\,381r^2+159\,915r^4-159\,579r^6$$
$$+91\,602r^8-33\,075r^{10}+7434r^{12}-945r^{14}+29r^{16})$$
$$+\frac{c}{160\times48^3}(86r^2-168r^4+105r^6-24r^8+r^{10}).$$

It is apparent that w_{000} and η_{000} give the velocity and temperature distributions in a stationary straight tube. The results (38), (43), (50) and (53) are the corresponding solutions for a stationary curved tube calculated in ref. [12]. And the solutions (39), (44), (51) and (54) are in agreement with ref. [13].

Similarly, we may obtain higher order solutions. However, the amount of labour required is considerable. Also it is hard to tell under what conditions the higher order solutions are needed until we get enough terms to unveil the analytic structure of the solution. Usually a perturbation solution is carried to the second approximation. Now, the routine labour of calculating higher approximations may be delegated to a computer. Then, dozens or even hundreds of terms may typically be found. These may suffice to permit the structure of the solution to be analyzed for a single power series, and the solution may be improved to extend its utility [8, 9]. Unfortunately, there is no such approach available at the present time for analyzing the multiple series in this problem. Besides, even for single power series, we must obtain the first few terms of the solution by hand in order to use computer to obtain higher order solutions.

It should be noted that the solutions of ϕ, w and η reduce to the corresponding ones of the six special

cases by setting any one or two of σ, Re_Ω and Ra_Ω to be zero. They are Dean problem, Coriolis problem, mixed convection problem, Dean problem with the effect of rotation, Dean problem with the effect of heating/cooling and Coriolis problem with the effect of heating/cooling.

3. RESULTS AND DISCUSSION

3.1. *Flow transitions in secondary flow*

3.1.1. *First-order approximation.* To the first-order of approximation, the secondary flow pattern is determined by ϕ_1 (equation (41)). ϕ_1 reaches its extreme values under the conditions

$$\frac{\partial \phi_1}{\partial r} = \frac{\partial \phi_1}{\partial \varphi} = 0$$

which requires

$$7(1-L_2)r^4 - (24+5L_1-53L_2)r^2 + (4+L_1-10L_2) = 0 \quad (69)$$

$$\sin \varphi = 0. \quad (70)$$

According to the definition of stream function (equation (4)) and the extreme conditions, both the radial and tangential components of the velocity in the cross-section vanish at the extreme points. The streamlines of motion through these points are circles (in a plane parallel to the axis of the tube) with the centres located at the axis of the rotation of the tube. The motion of the fluid may then be regarded as screw motions about these circular streamlines. In other words, the locations of the extreme points of ϕ_1 represent the centres of the screw motion of the fluid. The extreme values, on the other hand, have two implications. Their absolute values reflect the strength of the secondary flow, and their sign denotes the direction of the screw motion, namely, positive for counter-clockwise circulation and negative for clockwise circulation.

The locations of the extreme points are determined by the solutions of the equations (69) and (70). Equation (70) has two solutions in the flow domain $0 \leqslant \varphi < 2\pi$, namely, $\varphi = 0$ and $\varphi = \pi$. Thus, all extreme points are located along the vertical centreline.

The radial distance of the extreme points is determined by the solutions of the equation (69) which depend on the two dimensionless parameters, namely, L_1 and L_2. For some L_1 and L_2, equation (69) has only one solution (r_{1m}) which gives a minimum value of ϕ_1 with a negative sign. For some other L_1 and L_2, equation (69) has only one solution (r_{2m}) which yields a maximum value of ϕ_1 with a positive sign. For still other L_1 and L_2, equation (69) has two solutions (r_{1m} and r_{2m}) which result in a minimum value of ϕ_1 with a negative sign and a maximum value of ϕ_1 with a positive sign, respectively. The structure of the solution is summarized in Table 1. The readers are referred to ref. [7] for a detailed analysis on the variations of r_{1m} and r_{2m} with L_1 and L_2.

Table 1 shows that in the laminar flow region, the secondary flow experiences two transitions which occur at $L_1 = 10L_2-4$ and $L_1 = 9L_2-3$, respectively. Consequently, the secondary flow appears as three different patterns, namely, two cells of counter-clockwisely circulating vortices; two cells of clockwisely circulating vortices; and two-pairs (four cells) of counter-rotating vortices which are directed opposite to each other.

Typical secondary flow patterns are illustrated in the first column of Fig. 2. The symmetry about the horizontal centreline allows us to show the upper half of the cross-section only. In the figure, the stream function is normalized by its maximum absolute value. The cross denotes the position at which the stream function reaches its maximum absolute value. And two numbers for each case are the value of the L_1 and the extreme value of the stream function which yields the maximum absolute value. A vortex with a positive (negative) value of the stream function indicates a counter-clockwise (clockwise) circulation.

When $L_1 \geqslant 9L_2-3$ and $L_2 \leqslant 1$ or $L_1 \geqslant 10L_2-4$ and $L_2 \geqslant 1$, the secondary flow appears as two-cell, counter-rotating vortices as shown in Fig. 2(a, b). When L_1 is in the region $10L_2-4 < L_1 < 9L_2-3$ and $L_2 \leqslant 1$ or $9L_2-3 < L_1 < 10L_2-4$ and $L_2 \geqslant 1$, the secondary flow appears as two pairs (four cell) of counter-rotating vortices, with one pair in clockwise circulation and the other in counterclockwise circulation [Fig. 2(c,d)]. When $L_1 \leqslant 10L_2-4$ and $L_2 \leqslant 1$ or $L_1 \leqslant 9L_2-3$ and $L_2 \geqslant 1$, however, the secondary flow becomes two cell counter-rotating vortices again, but with the direction of clockwise circulation as shown in Fig. 2(e, f).

Three points are worthy of mention regarding the four cell vortex structure [Fig. 2(c, d)]: (1) this structure is qualitatively different from the four cell vortex families encountered in Dean, Coriolis or mixed convection problems. (2) Its strength is very weak. This can be inferred from the maximum absolute value of the stream function. The analysis of force mechanism suggests that the centrifugal, Coriolis and buoyancy forces, overall, just neutralize each other in this region. (3) The clockwise circulating vortices occur near the tube wall if $L_2 \leqslant 1$ [Fig. 2(c, d)]. If $L_2 \geqslant 1$, however, they will appear in the central position of the cross-section of the tube as shown in Fig. 2(g).

For an isothermal flow in a rotating curved channel without effect of heating/cooling, the stability analysis made in ref. [14] concludes that there exist two potentially unstable regions separated by two stable regions in the cross-plane when the flow is in the region with four cell secondary flow structure. Visualization of the secondary flow in a rotating curved square channel in ref. [14] explored a similar structure as the four cell structure found in the present work.

3.1.2. *Second-order approximation.* The second col-

Table 1. Distribution of the solution with L_1 and L_2

		$L_2 \leqslant 1$	
Region	$L_1 \leqslant 10L_2-4$	$10L_2-4 \leqslant L_1 \leqslant 9L_2-3$	$L_1 \geqslant 9L_2-3$
Solution	r_{1m}	r_{1m} and r_{2m}	r_{2m}
		$L_2 \geqslant 1$	
Region	$L_1 \leqslant 9L_2-3$	$9L_2-3 \leqslant L_1 \leqslant 10L_2-4$	$L_1 \geqslant 10L_2-4$
Solution	r_{1m}	r_{1m} and r_{2m}	r_{2m}

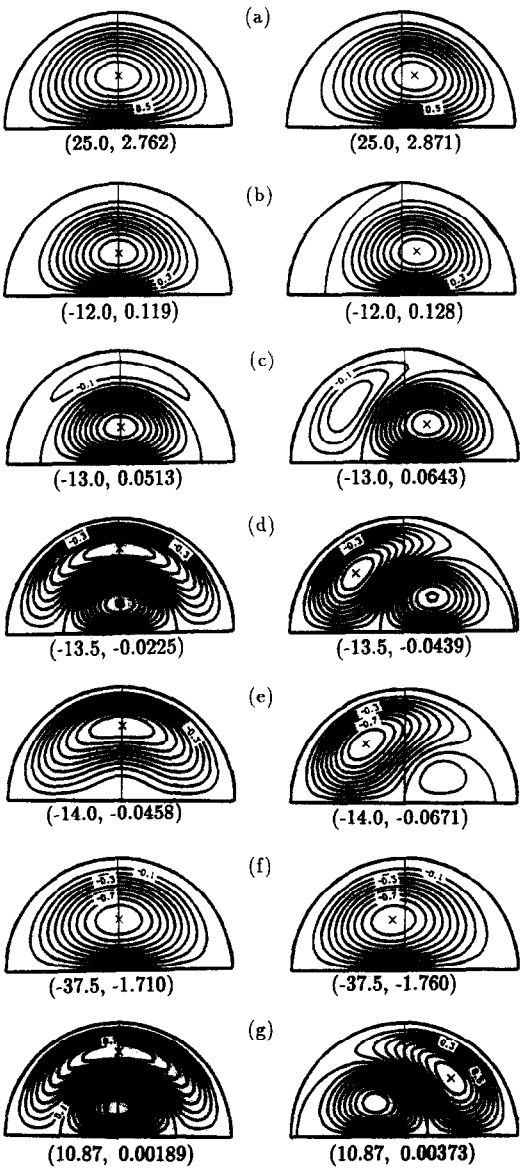

Fig. 2. Secondary flow patterns: (a–f) at $\sigma = 0.02$, $Pr = 0.7$, $c = 60$ and $L_2 = -1.0$; (g) at $\sigma = 0.01$, $Pr = 0.7$, $c = 50$ and $L_2 = 1.5$ (first column: first-order; second column: second-order).

umn in Fig. 2 illustrates the secondary flow patterns based on full second-order approximation. The corresponding first-order secondary flow patterns are shown in the first column of the figure. A striking feature is that the symmetry about the vertical centreline exhibited in the first-order secondary flow breaks down with the circulation centre of vortices shifting away from the vertical centreline. Also the corresponding vortices are distored in some ways. In particular, the circulation centre for all clockwise circulation vortices moves inward and downward, while that for all counter-clockwise circulation vortices moves outward and upward with the exception of that in Fig. 2(g). This trend is also more noticeable in the region with four cell patterns. Another interesting feature is that the region with four cell secondary flow is wider than that of the corresponding first-order secondary flow.

Three factors contribute to the generation of the secondary flow in this problem: curvature, rotation and heating/cooling. The secondary flow patterns discussed in Fig. 2 result from the combined effect of all these three factors. The analytical solutions, however, allow us to visualize the secondary flow due to one or any two of these three factors simply by setting some terms in the series to be zero. In other words, the solutions can be used to analyse the secondary flows for several special cases. They are secondary flows in curved tubes (classical Dean problem), radially rotating tubes (Coriolis problem), stationary straight tubes with heating/cooling (mixed convection problem), rotating curved tubes, curved tubes with heating/cooling and radially rotating straight tubes with heating/cooling. Figure 3 is one set of such secondary flows, which exhibit several interesting features to be noted below.

All the first-order terms in the series result in a symmetric (about vertical centreline) one pair-counter-rotating secondary flow with the centres of circulation located on the vertical centreline. Note that the first order approximation is valid for sufficiently small values of the dynamical parameters, the structure of the fully developed secondary flow in Dean problem, Coriolis problem and mixed-convection problem, then, consists of one pair (two cell) counter-rotating vortices with one cell located in the upper half and another in the lower half of the cross-section at sufficiently small values of the dynamical parameters. They are also symmetric about the vertical centreline. This is in agreement with the previous works for the corresponding problems.

All the second-order terms in the series of the stream function cause the secondary flow to exhibit a four cell pattern with the centre of the circulation away from the vertical centreline. It is interesting to note

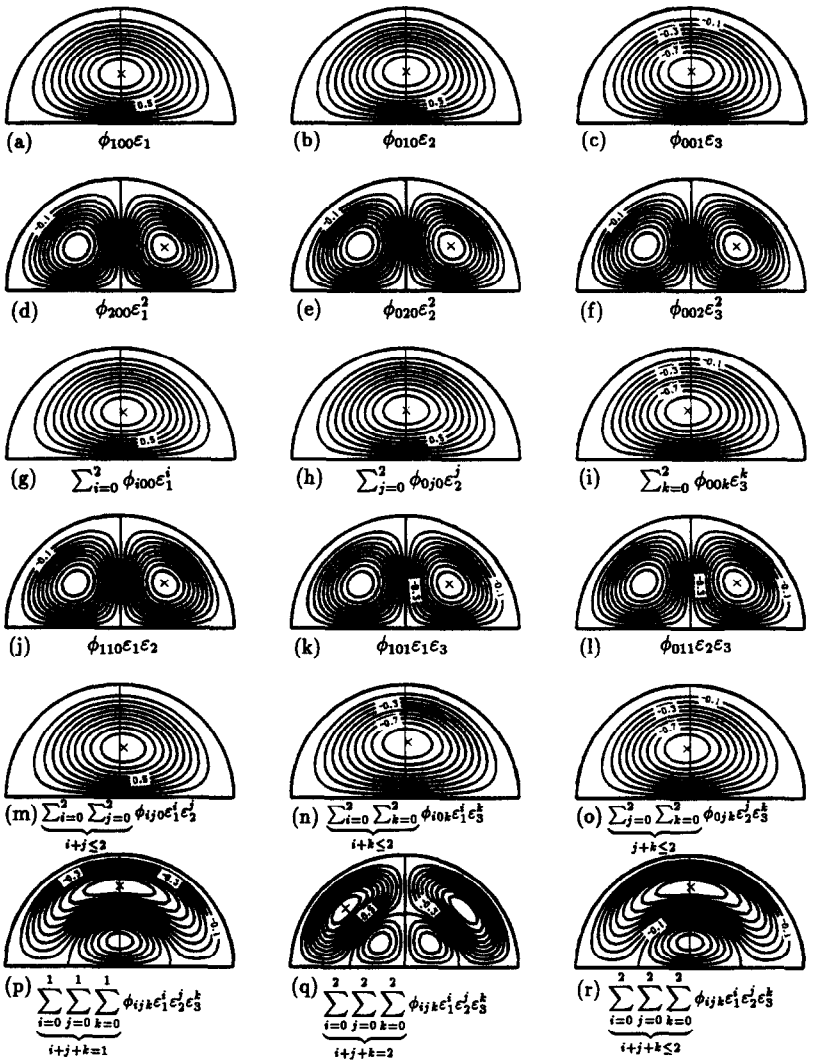

Fig. 3. Secondary flow with one, two or three effects of curvature, rotation and heating/cooling at $\sigma = 0.01$, $Pr = 0.7$, $c = 100$, $L_1 = 1.1$ and $L_2 = 0.5$ [(a–c) first-order terms due to single effect of curvature, rotation and heating/cooling; (d–f) second-order terms due to single effect of curvature, rotation and heating/cooling; (g–i) first-order terms + second-order terms due to single effect of curvature, rotation and heating/cooling; (j–l) second-order terms due to combined effect of curvature and rotation, curvature and heating/cooling and rotation and heating/cooling; (m–o) first-order terms + second-order terms due to combined effect of curvature and rotation, curvature and heating/cooling and rotation and heating/cooling; (p–r) first-order terms, second-order terms and first-order terms + second-order terms due to combined effect of all three factors].

that the secondary flow due to the second-order term itself is still symmetric about the vertical centreline. The symmetry is, however, lost in the secondary flow resulting from all the first-order and second-order terms in the series. This breakdown of the symmetry comes from the asymmetric effect of second-order terms on the first-order terms about the vertical centreline, i.e. the secondary flow of the second-order terms enhances that of the first-order terms on one side of the vertical centreline, but neutralizes it on the other side of the centreline.

The secondary flow with the simultaneous effect of more than one factor of curvature, rotation and heating/cooling may be qualitatively similar to or completely different from that with only one factor depending on the region of the governing parameters.

3.2. *Flow transitions in main flow*

Figure 4 shows several typical main flow isovels and profiles based on the second-order approximation. The corresponding secondary flows are shown in Fig. 2. Once again, the symmetry of flow about the horizontal centreline allows us to show the upper half of the cross-section only. A cross in the figure denotes the position at which the main flow reaches its maximum value. The value of L_1 and the maximum value of the main velocity are given in the figure for each case.

Some features of the main flow can be expected and

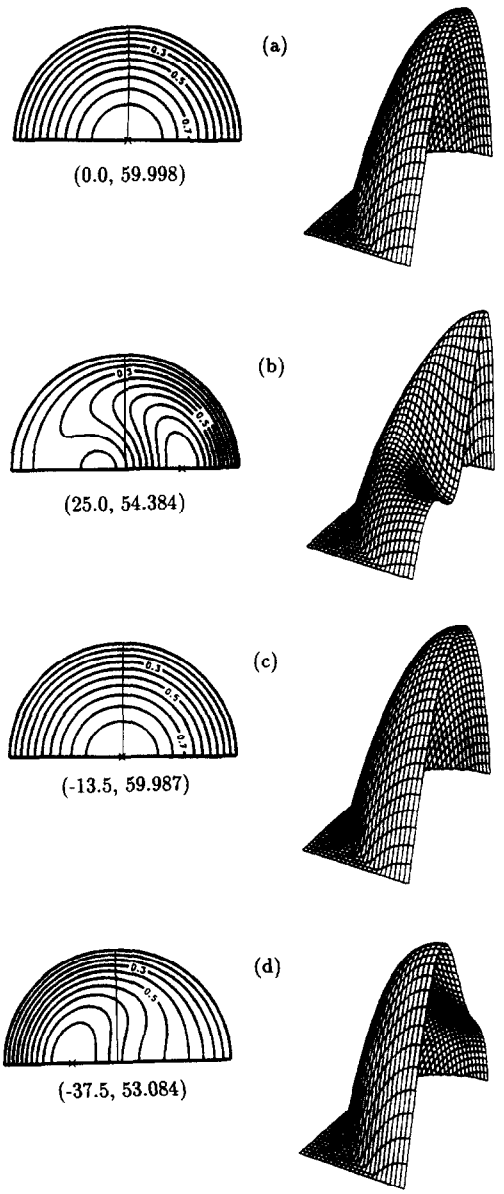

Fig. 4. Main velocity distributions at $\sigma = 0.02$, $Pr = 0.7$, $c = 60$ and $L_2 = -1.0$ (first column: isovels; second column: profiles).

understood through the force balance in the governing equation. It is the secondary flow that causes the deviation of the main flow away from the parabolic profile in Poiseuille flow. The secondary flow affects the main flow through three terms: the convection term, and two Coriolis terms due to the curvature and rotation, respectively. The two Coriolis terms may be in the same direction or opposite to the main flow depending on the sign of $U\sin\varphi + V\cos\varphi$ and Ω. The absence of these three terms leads to the Poiseuille solution with an axisymmetric and parabolic profile [Fig. 4(a)]. The relative importance of the different terms depends on the magnitudes of the governing parameters, and shows different flow patterns for different regions. The driving term is the axial pressure gradient which is always important. The viscous term is always important near the wall, but may not be significant in the core region for certain ranges of the parameters. If the rotation speed is high enough, the Coriolis terms could be of the same order of magnitude as that of the pressure gradient term. The main flow would, then, exhibit a geostrophic pattern in the centre of the cross-section surrounded by a thin boundary layer according to the theory of rotating fluid [15]. This is one limiting case examined in refs. [3, 4].

As discussed in Section 3.1, secondary flow is very weak in the region where centrifugal, Coriolis and buoyancy forces just neutralize each other. Consequently, it is too weak to modify the main flow effectively such that the profiles of the main flow are essentially axisymmetric and parabolic with the maximum value occurring along the horizontal centreline at or very close to the centre of the cross-section [Fig. 4(c)]. In this region, the inertial force in equation (2) is very weak as compared with the viscous force. The driving force for the main flow (i.e. pressure term) is mainly balanced by the viscous force in whole flow domain. Other forces (inertial, Coriolis forces) are very weak.

When the value of L_1 is away from the region where the centrifugal, Coriolis and buoyancy forces just neutralize each other, the secondary flow becomes stronger (Fig. 2). The profile of the main flow becomes, then, distorted with the peak moving away from the centre of the cross-section toward the outer wall for the case of increasing value of L_1 [Fig. 4(b)] or the inner wall for the case of decreasing value of L_1 [Fig. 4(d)] along the horizontal centreline. In either of the two cases, the location of the maximum main velocity is away from the centre of the tube and in the direction of the secondary velocities in the middle of the tube. Due to the shift of the peak of the main flow, the isovels are more sparsely spaced in the region near the inner wall (outer wall) than near the outer wall (inner wall) in Fig. 4(b) [Fig. 4(d)]. Consequently, pronounced peripheral variations are expected in the local friction factors. The flow in the tube core is not geostrophic, it is ageostrophic, i.e. the pressure gradients are balanced by both Coriolis force and convective inertial force.

A striking feature which can be inferred from Fig. 4(a–d) is that the region of return flow along the walls appears to be far too thick to be described by boundary layer approximations. Consequently, the integral type method developed by Mori *et al.* [16, 17] may not be valid for these regions of flow.

3.3. *Temperature distribution*

Figure 5 demonstrates the way in which the secondary flow affects the temperature profiles based on the second-order solution of the temperature. In the figure, the nondimensional temperature η has been normalized by its corresponding extreme value η_e, and the extreme point is illustrated by a cross. Two numbers for each case are, respectively, the value of the L_1 and the extreme value of η.

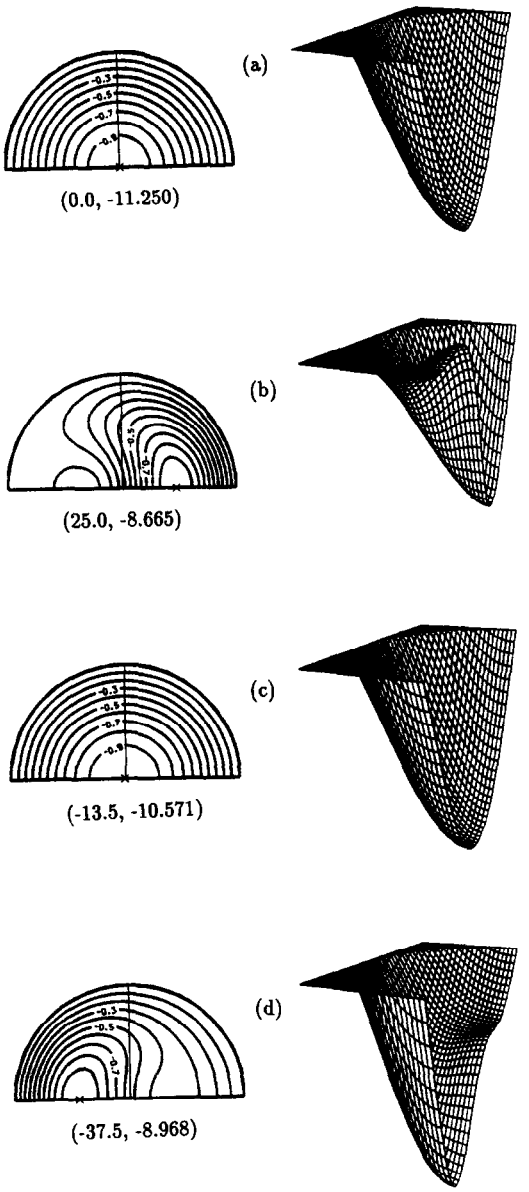

Fig. 5. Temperature distributions at $\sigma = 0.02$, $Pr = 0.7$, $c = 60$ and $L_2 = -1.0$ (first column: isothermals; second column: profiles).

It is the secondary flow that causes the deviation of the temperature from the parabolic profile in the stationary straight tubes. The effect of the secondary flow enters the energy equation through one term, i.e. the convection term. The absence of this term leads to the parabolic profile which has an axisymmetric and parabolic profile [Fig. 5(a)]. In the region with the four cell secondary flow, the secondary flow is too weak to modify the temperature distributions effectively. Consequently, the temperature profile in this region exhibits essentially axisymmetric and parabolic with an extreme value appearing along the horizontal centreline, at, or very close to, the centre of the cross-section [Fig. 5(c)].

When L_1 moves away from this region in both directions, the stronger secondary flow causes the temperature profile to be distorted with the extreme point shifting from the centre of the cross-section to the outer wall for the case of increasing L_1 [Fig. 5(b)] or to the inner wall for the case of decreasing L_1 [Fig. 5(d)] along the horizontal centreline. The shift of the extreme point results in a more tightly spaced isotherms in the region near the outer wall [Fig. 5(b)] or near the inner wall [Fig. 5(d)]. This results from the larger gradient of the main flow in these regions [Fig. 4(b, d)] and will cause pronounced peripheral variations in the local Nusselt number.

Two interesting results can be inferred from the temperature profiles shown in Fig. 5(a–d). One is that the theory of thermal boundary layer is not valid for the temperature fields in these regions of the parameters because the layer along the walls is too thick to be described by the theory. Another is that the temperature distributions are qualitatively similar to the corresponding ones of the main flow. This implies that the Coriolis terms in the momentum equation for main flow are not strong enough to dominante in these regions of the parameters, by noting that only difference between the momentum equation for main flow and energy equation for temperature is the existence of the Coriolis terms in the momentum equation.

3.4. *Mean friction factor and Nusselt number*

3.4.1. *The friction factor.* Substituting the expression for w, based on a second-order solution, into the definition of flow rate Q

$$Q = \int_0^{2\pi}\int_0^{a} WR\,\mathrm{d}R\,\mathrm{d}\varphi = \int_0^{2\pi}\int_0^{1} avwr\,\mathrm{d}r\,\mathrm{d}\varphi$$

we obtain

$$Q = \frac{\pi vac}{2} Q_1, \tag{71}$$

where

$$\begin{aligned} Q_1 = 1 &- \left(\frac{1541c^4}{3150\times 1152^2} + \frac{11c^2}{17\,280} - \frac{1}{48}\right)\sigma^2 \\ &- \left(\frac{c^2}{28\times 768^2} + \frac{1}{9216}\right) Re_\Omega^2 - \frac{5293c^2 Ra_\Omega^2}{350\times 1152^3} \\ &- \left(\frac{111c^2}{280\times 1152^2} + \frac{1}{1920}\right) c\sigma Re_\Omega + \left(\frac{8077c^2}{50\,400\times 1152^2}\right. \\ &\left. + \frac{29}{240\times 1152}\right) c\sigma Ra_\Omega + \left(\frac{97c^2}{430\,080\times 4608}\right. \\ &\left. + \frac{1}{23\,040}\right) Re_\Omega Ra_\Omega \end{aligned} \tag{72}$$

and the mean main velocity w_m is

$$w_m = \frac{Q}{\pi a^2} = \frac{vcQ_1}{2a}. \tag{73}$$

Then the Reynolds number with the diameter of the tube as a characteristic length is

$$Re = \frac{2w_m a}{\nu} = cQ_1. \tag{74}$$

From equation (49), the flow rate of the fluid through a stationary straight tube is

$$Q_s = \frac{\pi \nu a c}{2}.$$

Then we may define the ratio of the flow rates as

$$\frac{Q}{Q_s} = Q_1. \tag{75}$$

This agrees with those in refs. [12, 13, 18] for the special cases they considered.

Since the mean friction factor for a rotating curved tube is defined by

$$f = -\frac{2a}{\rho w_m^2/2}\frac{\partial p'}{R\partial\theta}$$

we have

$$\frac{f}{f_s} = \frac{c}{Re} = \frac{1}{Q_1}, \tag{76}$$

where $f_s(= 64/Re)$ is the mean friction factor for a stationary straight tube. It is interesting to note that Prandtl number does not appear explicitly in the expressions of Q/Q_s and f/f_s, although it was present in the second-order solution of the main velocity.

Figure 6(a) illustrates the typical trends for the friction factor variation with L_1 and L_2 at $\sigma = 0.02$ and $c = 60$. For any specified L_2, there exists a region of L_1 where the friction factor is identical or very close to that in a stationary straight tube when centrifugal, Coriolis and buoyancy forces just neutralize each other. As L_1 moves away from this region at a specified value of L_2, the friction factor increases. Apparently the increased resistance to the flow results from the stonger secondary flow. Furthermore, the increase in friction factor becomes more significant as $|L_1|$ increases. At a specified value of L_1, the flow impediment at higher values of L_2 is relatively greater if the value of L_1 is at the left of the low friction factor region, but is relatively smaller if the value of L_1 is at the right of the region.

3.4.2. *The Nusselt number.* Energy balance

$$\rho c_p c_2 \pi a^2 w_m = 2\pi a h(t_w - t_m)$$

and the definition of the mean Nusselt number

$$Nu = \frac{2ah}{\lambda}$$

yield

$$Nu = \frac{cQ_1}{2\eta_m} \tag{77}$$

in which η_m is an integrated mean temperature across

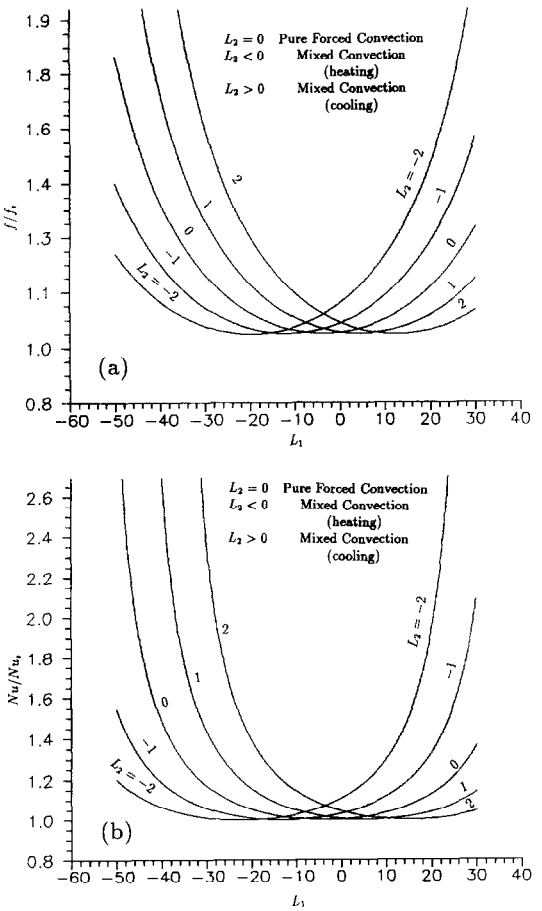

Fig. 6. The influence of secondary flow on flow resistance and heat transfer.

the tube (sometimes referred to as an unweighed mean) and defined as [1]

$$\eta_m = \frac{1}{\pi}\int_0^{2\pi}\int_0^1 \eta r\,dr\,d\varphi.$$

Substituting the second-order solution of η into the expression above yields

$$\eta_m = -\frac{c}{12} + \sigma^2\left(\frac{1171Pr^2c^5}{22400\times1152^2} + \frac{4169Prc^5}{5\times50400\times1152^2} + \frac{1171c^5}{22400\times1152^2} - \frac{17Prc^3}{6720\times1152} + \frac{481c^3}{6720\times1152} - \frac{29c}{1536}\right) + Re_\Omega^2\left(\frac{17Pr^2c^3}{2293760\times1152} + \frac{293Prc^3}{107520\times1152^2} + \frac{17c^3}{2293760\times1152} + \frac{c}{80\times1152}\right) + Ra_\Omega^2\left(\frac{72143Pr^2c^3}{44800\times1152^3}\right.$$

$$+\frac{57\,383Prc^3}{112\,000\times1152^3}+\frac{72\,143c^3}{44\,800\times1152^3}\Bigg)$$

$$+\sigma Re_\Omega\left(\frac{2129Pr^2c^4}{50\,400\times1152^2}+\frac{2707Prc^4}{201\,600\times1152^2}\right.$$

$$\left.+\frac{2129c^4}{50\,400\times1152^2}-\frac{Prc^2}{960\times1152}+\frac{19c^2}{320\times1152}\right)$$

$$-\sigma Ra_\Omega\left(\frac{27\,571Pr^2c^4}{1400\times1152^3}+\frac{7291Prc^4}{1\,344\,000\times1152^2}\right.$$

$$\left.+\frac{27\,571c^4}{1400\times1152^3}-\frac{Prc^2}{2\,752\,512}+\frac{253c^2}{21\,504\times1152}\right)$$

$$-Re_\Omega Ra_\Omega\left(\frac{11\,143Pr^2c^3}{1400\times1152^3}+\frac{3551Prc^3}{1400\times1152^3}\right.$$

$$\left.+\frac{11\,143c^3}{1400\times1152^3}+\frac{77c}{3840\times4608}\right). \tag{78}$$

The following implication of equations (77) and (78) is worthy of note. In the limiting case with no curvature, rotation and heating/cooling, the present problem becomes identical to the asymptotic solution for constant property forced convection in a stationary straight tube and was reported in ref. [19]. For this limiting case $Nu_s = 6$ and clearly equation (77) approaches to this value asymptotically as $\sigma \to 0$, $Re_\Omega \to 0$ and $Ra_\Omega \to 0$. Dividing equation (77) by Nu_s for a stationary straight tube, we have

$$\frac{Nu}{Nu_s} = \frac{11cQ_1}{96\eta_m}. \tag{79}$$

Typical variations of the Nusselt number given by equation (79) are presented in Fig. 6(b) for a range of L_2 at $\sigma = 0.02$, $c = 60$, and $Pr = 0.7$. Although it is likely that the solution is being extended beyond its range of validity at the higher values of L_1, the physical trends are quite evident. As expected, the heat transfer is enhanced significantly due to the presence of the secondary flow, and the similarity between the main flow and temperature distribution leads to a similarity in the results for friction factor and Nusselt number. Like the friction factor, the Nusselt number is also identical or very close to that for constant property forced convection in a stationary straight tube in the region with the four-cell secondary flow. An increase in $|L_1|$ from this region causes the secondary flow to become stronger. Consequently, the Nusselt number increases substantially at higher values of the $|L_1|$. The higher value of L_2 leads to a relatively greater enhancement of heat transfer for the case in which the value of L_1 is at the left of the region with the lowest value of the Nusselt number, but a relatively smaller enhancement when the value of L_1 is at the right of the region.

At the present stage, the structure of the solutions has not been explored completely. On the other hand, it appears that no experimental results of friction factors or Nusselt numbers for a rotating curved tube with heating or cooling effect are available. Thus, the range of validity for equations (76) and (79) remains to be checked in future.

3.5. *Structure of solutions*

In practical problems, the Reynolds number Re is usually given, while the pseudo Reynolds number c, which is defined by the pressure gradient along curved tube axis, is often unknown. An expression for the pseudo Reynolds number c in terms of Re, σ, Re_Ω and Ra_Ω may be obtained by inverting equation (74) and ignoring the higher-order terms as

$$c = Re\Gamma \tag{80}$$

with

$$\Gamma = 1+\left(\frac{1541Re^4}{3150\times1152^2}+\frac{11Re^2}{17\,280}-\frac{1}{48}\right)\sigma^2$$

$$+\left(\frac{Re^2}{28\times768^2}+\frac{1}{9216}\right)Re_\Omega^2+\frac{5203Re_\Omega^2Ra_\Omega^2}{350\times1152^3}$$

$$+\left(\frac{111Re^2}{280\times1152^2}+\frac{1}{1920}\right)\sigma ReRe_\Omega-\left(\frac{8077Re^2}{50\,400\times1152^2}\right.$$

$$\left.+\frac{29}{240\times1152}\right)\sigma ReRa_\Omega-\left(\frac{97Re^2}{430\,080\times4608}\right.$$

$$\left.+\frac{1}{23\,040}\right)Re_\Omega Ra_\Omega. \tag{81}$$

Introducing the following nondimensional parameters:

$$De = Re\sqrt{\sigma};\quad D_\Omega = ReRe_\Omega;\quad Dr = ReRa_\Omega \tag{82}$$

the expression of Γ becomes

$$\Gamma = 1-\frac{\sigma^2}{48}+\frac{1541(De^2)^2}{3150\times1152^2}+\frac{D_\Omega^2}{28\times768^2}$$

$$+\frac{5293Dr^2}{350\times1152^3}+\frac{Re_\Omega^2}{9216}+\frac{11\sigma De^2}{17\,280}+\frac{\sigma D_\Omega}{1920}$$

$$-\frac{29\sigma Dr}{240\times1152}+\frac{111De^2D_\Omega}{280\times1152^2}-\frac{8077De^2Dr}{50\,400\times152^2}$$

$$-\frac{97D_\Omega Dr}{430\,080\times4608}-\frac{Re_\Omega Dr}{23\,040Re}. \tag{83}$$

The second-order solution (8) along with equations (38)–(68), may be expressed as

$$\phi = \hat{De}^2\phi_{100}^{20}+\hat{D}_\Omega^2\phi_{010}^{10}+\hat{Dr}^2\phi_{001}^{10}+\hat{De}^4\phi_{200}^{40}$$

$$+\hat{D}_\Omega^2\phi_{020}^{20}+\hat{Dr}^2\phi_{002}^{20}+\sigma\hat{De}^2\phi_{200}^{20}+\sigma\hat{D}_\Omega^2\phi_{110}^{10}$$

$$+\sigma\hat{Dr}^2\phi_{101}^{10}+\hat{De}^2\hat{D}_\Omega\phi_{110}^{30}+\hat{De}^2\hat{Dr}\phi_{101}^{30}+\hat{D}_\Omega\hat{Dr}\phi_{010}^{20}$$

$$+ Pr\hat{D}e^2\hat{D}r\phi_{101}^{31} + Pr\hat{D}_\Omega\hat{D}r\phi_{011}^{21} + Pr\hat{D}r^2\phi_{002}^{21} \quad (84)$$

$$w = \hat{R}e[w_{000}^{10} + \sigma w_{100}^{10} + \hat{D}e^2 w_{100}^{30} + \hat{D}_\Omega w_{010}^{20} + \hat{D}r w_{001}^{20} + \sigma^2 w_{200}^{10} + \hat{D}e^4 w_{200}^{50} + Re_\Omega^2 w_{020}^{10} + \hat{D}_\Omega^2 w_{020}^{30} + \hat{D}r^2 w_{002}^{30} + \sigma\hat{D}e^2 w_{200}^{30} + \sigma\hat{D}_\Omega w_{110}^{20} + \sigma\hat{D}r w_{101}^{20} + \hat{D}e^2\hat{D}_\Omega w_{110}^{40} + \hat{D}e^2\hat{D}r w_{101}^{40} + \hat{D}_\Omega\hat{D}r w_{011}^{30} + Pr\hat{D}e^2\hat{D}r w_{101}^{41} + Pr\hat{D}r^2 w_{002}^{31} + Pr\hat{D}_\Omega\hat{D}r w_{011}^{31}] + Re_\Omega\hat{D}r w_{011}^{10} + \hat{D}r^2 w_{002}^{20} \quad (85)$$

$$\eta = \hat{R}e[\eta_{000}^{10} + \sigma\eta_{100}^{10} + \hat{D}e^2\eta_{100}^{30} + \hat{D}_\Omega\eta_{010}^{20} + \hat{D}r\eta_{001}^{20} + \sigma^2\eta_{200}^{10} + \hat{D}e^4\eta_{200}^{50} + Re_\Omega^2\eta_{020}^{10} + Re_\Omega^2 w_{020}^{10} + \hat{D}_\Omega^2\eta_{020}^{30} + \hat{D}r^2\eta_{002}^{30} + \sigma\hat{D}e^2\eta_{200}^{30} + \sigma\hat{D}_\Omega\eta_{110}^{20} + \sigma\hat{D}r\eta_{101}^{20} + Pr\hat{D}e^2\eta_{100}^{31} + Pr\hat{D}_\Omega\eta_{010}^{21} + Pr\hat{D}r\eta_{001}^{21} + \hat{D}e^2\hat{D}_\Omega\eta_{110}^{41} + \hat{D}e^2\hat{D}r\eta_{110}^{40} + \hat{D}_\Omega\hat{D}r\eta_{011}^{30} + Pr\hat{D}e^4\eta_{200}^{51} + Pr\hat{D}_\Omega^2\eta_{020}^{31} + Pr\hat{D}r^2\eta_{002}^{31} + \sigma Pr\hat{D}e^2\eta_{200}^{31} + \sigma Pr\hat{D}_\Omega\eta_{110}^{21} + \sigma Pr\hat{D}r\eta_{110}^{21} + Pr\hat{D}e^2\hat{D}_\Omega\eta_{110}^{41} + Pr\hat{D}e^2\hat{D}r\eta_{110}^{41} + Pr\hat{D}_\Omega\hat{D}r\eta_{011}^{31} + Pr^2\hat{D}e^4\eta_{200}^{52} + Pr^2\hat{D}_\Omega^2\eta_{020}^{32} + Pr^2\hat{D}r^2\eta_{002}^{32} + Pr^2\hat{D}e^2\hat{D}_\Omega\eta_{110}^{42} + Pr^2\hat{D}e^2\hat{D}r\eta_{110}^{42} + Pr^2\hat{D}_\Omega\hat{D}r\eta_{011}^{32}] + Re_\Omega\hat{D}r\eta_{011}^{10} + \hat{D}r^2\eta_{002}^{20} \quad (86)$$

in which

$$\hat{R}e = Re\Gamma; \quad \hat{D}e = De\Gamma; \quad \hat{D}_\Omega = D_\Omega\Gamma; \quad \hat{D}r = Dr\Gamma \quad (87)$$

and the parameter-free expansion coefficients ϕ_{ijk}^{lm}, w_{ijk}^{lm} and η_{ijk}^{lm} are introduced by factoring out the parameters c and Pr from ϕ_{ijk}, w_{ijk} and η_{ijk}, i.e.

ϕ_{ijk}^{lm} = items in ϕ_{ijk} including ith power of c and jth power of Pr divided by $c^i Pr^j$.

A similar remark is also true for w_{ijk}^{lm} and η_{ijk}^{lm}. Thus ϕ_{ijk}^{lm}, w_{ijk}^{lm} and η_{ijk}^{lm} depend on r and φ only and are independent of the flow region, i.e. the relative size of each term in these series depends on the magnitudes of the parameters, but the shape of each term is always the same. Note that Re is fixed once De and σ are specified, the solutions for velocity and temperature may be regarded as the infinite series (higher-order approximations would produce additional types of terms) in powers of σ, $\hat{D}e^2$, Re_Ω, $\hat{D}_\Omega$, Pr and $\hat{D}r$. In view of the expressions (82) and (83) for Γ (in fact $\Gamma \simeq 1$ for small values of the parameters), the series may also be considered as in powers of σ, De^2, Re_Ω, D_Ω, Pr and Dr.

The first pair of parameters, σ and De^2, characterizes the flow and heat transfer in stationary helically coiled tubes (the Dean problem). The second pair, Re_Ω and D_Ω, determines the characteristics of the flow and heat transfer in radially rotating straight tubes (the Coriolis problem). The third pair, Pr and Dr, characterizes the flow and heat transfer due to the inertial and buoyancy forces (the mixed convection problem). σ, the curvature ratio of the curved tube, is important for the problems in the helical tube with tightly wound coils. Dean number, De, characterizes the flow and heat transfer in the coiled tubes with loosely wound coils. Re_Ω, whose effect for problems in radially rotating straight tube is analogous to that of σ for the stationary curved tube, is the ratio of the Coriolis force to the viscous force. It is important for problems in the radially rotating tube if D_Ω is small. D_Ω, whose effect for the problems in the radially rotating straight tube is analogous to that of the square of the Dean number for the stationary curved tube, represents the ratio of the product of the inertial and Coriolis forces to the square of the viscous forces. It determines the flow and heat transfer in the radially rotating straight tube if Re_Ω is small (i.e. slowly rotating). Dr represents the ratio of the product of the inertial and buoyancy forces to the square of the viscous forces. Dr and Prandtl number Pr are two characteristic parameters for the mixed convection problem.

If each of these parameters is significant, the solution becomes a sixfold series expansion in σ, De, Re_Ω, D_Ω, Pr and Dr. It appears that no successful technique is available for analyzing and improving such a multiple series. However, for some special cases, the series may be reduced to a single series. For example, the solution series for the fully developed steady laminar flow through a radially rotating straight tube becomes a single series if the tube is rotating slowly and the density of the fluid is taken to be constant. Mansour [20] expanded this single series up to 34 terms in powers of D_Ω. Recasting the resulting series for the friction ratio, he predicted that it will grow asymptotically as the 1/8 power of D_Ω. Van Dyke [10] extended Dean's four-term series for the loosely coiled tube to 24 terms in power of De. The series, re-casted by Van Dyke, is considered to be valid for arbitrarily large Dean number. Similar work has been done by Van Dyke [11] for Morton's series for fully developed laminar flow through a uniformly heated horizontal tube. He extended the series by computer to 31 terms in powers of a parameter ε which is similar to Dr of this work. He found that the Nusselt number grows asymptotically as the 2/15 power of the parameter ε.

From the definition of L_1 and L_2 [equation (42)],

$$L_1 = \frac{3Re_\Omega}{2\sigma c} = \frac{3\hat{D}_\Omega}{2\hat{D}e^2}; \quad L_2 = \frac{Ra_\Omega}{16\sigma c} = \frac{\hat{D}r}{16\hat{D}e^2}. \quad (88)$$

Thus, L_1 represents the ratio of the characteristic parameter $\hat{D}_\Omega$ for the rotating straight tube to the characteristic parameter $\hat{D}e^2$ for the stationary curved tube. Similarly, L_2 represents the ratio of the characteristic parameter $\hat{D}r$ for the mixed heat transfer problem to

Table 2. Physical implications of $\hat{D}e^2$, $\hat{D}_\Omega$, $\hat{D}r$, L_1 and L_2

Parameter	Force ratio
$\hat{D}e^2(De^2)$	$\frac{\text{(inertial force)} \times \text{(centrifugal force)}}{\text{(viscous force)}^2}$
$\hat{D}_\Omega(D_\Omega)$	$\frac{\text{(inertial force)} \times \text{(Coriolis force)}}{\text{(viscous force)}^2}$
$\hat{D}r(Dr)$	$\frac{\text{(inertial force)} \times \text{(buoyancy force)}}{\text{(viscous force)}^2}$
L_1	$\frac{\text{Coriolis force}}{\text{centrifugal force}}$
L_2	$\frac{\text{buoyancy force}}{\text{centrifugal force}}$

the characteristic parameter $\hat{D}e^2$ for the stationary curved tube.

In terms of the force ratios, the physical implications of $\hat{D}e^2$, $\hat{D}_\Omega$, $\hat{D}r$, L_1 and L_2 are summarized in Table 2.

4. CONCLUDING REMARKS

For any continuous function of one or more variables, there exists a unique, uniformly convergent polynomial which can be used to approximate the function. Assuming that the stream function ϕ, the main velocity w and the temperature η are continuous on the curvature ratio σ, the rotational Reynolds number Re_Ω and the rotational Rayleigh number Ra_Ω, a systematic method is developed to determine an approximate analytical solution for velocity and temperature fields in a rotating curved tube under the conditions that the flow and temperature fields are fully developed, and the wall heat flux is uniform with peripherally uniform wall temperature.

Each of the functions ϕ, w and η is expanded in a triple power series in terms of σ, Re_Ω and Ra_Ω. The coefficients in these expansion series may be obtained from the solutions of the associated nonhomogeneous harmonic and biharmonic differential equations. In calculating each additional term of the series, the terms on the right hand sides of the harmonic and biharmonic differential equations, are in terms of the functions determined from the solution of the preceding harmonic and biharmonic differential equations. Therefore the successive solutions of the three main differential equations will produce as many terms as desired for the three series, depending upon the accuracy required. In this work, the solution is carried up to and including the second-order terms. As well, the analytical expressions for the velocity and temperature distributions are applicable for both heating and cooling cases with either positive or negative rotation. The solutions of velocity and temperature are found to be infinite series in powers of three pairs of parameters which characterize the Dean, the Coriolis and the mixed convection problems, respectively.

By setting any one or two of σ, Re_Ω and Ra_Ω to be zero, the solution reduces to the corresponding six special cases, i.e. the Dean problem, Coriolis problem, mixed convection problem, Dean problem with effect of rotation, Dean problem with effect of heating/cooling and Coriolis problem with effect of heating/cooling.

The centrifugal, Coriolis and buoyancy forces all contribute to the generation of the secondary flow in a rotating curved tube. The resultant secondary flow may be grouped under three broad patterns depending on the values of two dimensionless parameters L_1 and L_2. The first parameter represents the ratio of the characteristic dimensionless parameter $\hat{D}_\Omega$ for a radially rotating straight tube to the characteristic dimensionless parameter $\hat{D}e^2$ for a stationary curved tube. The last one, on the other hand, is the ratio of the characteristic dimensionless parameter $\hat{D}r$ for mixed convection to the $\hat{D}e^2$. The results presented here extend the range of parameters for which the flow in rotating curved tubes has been studied, especially as regards the secondary flow reversal and the four-cell flow structure.

The presence of the secondary flow causes the derivation of the main velocity and temperature profiles away from the parabolic profile in Poiseuille flow. In particular, the locations of the maximum main velocity and the extreme temperature are moved away from the centre of the tube in the direction of the secondary velocities in the middle of the tube. This results in a pronounced peripheral variation of friction factor and Nusselt number and a significant increase in the mean friction factor and Nusselt number. However, in the flow region with a four-cell structure, the secondary flow is too weak to modify the main velocity and temperature profiles effectively, such that the friction factor and Nusselt number are identical or very close to those for constant property forced convection in a stationary straight tube.

The profiles of the main velocity and temperature show that the boundary layer theory is not valid for the analysis of the flow and heat transfer in a rotating curved tube for a range of parameters considered in this work.

REFERENCES

1. W. D. Morris, *Heat Transfer and Fluid Flow in Rotating Coolant Channels*. Research Studies Press, Wiley, London (1981).
2. J. S. Papanu, R. J. Adler, M. B. Gorensek and M. M. Menon, Separation of fine particle dispersions using periodic flows in a spinning coiled tube, *AICHE J.* **32**, 798–808 (1986).
3. L. M. Hocking, Boundary and shear layers in a curved rotating pipe, *J. Math. Phys. Sci.* **1**, 123–136 (1967).
4. H. Ludwieg, Die ausgebildete kanalstromung in einem rotierenden system, *Ing.-Arch.* **19**, 296–308 (1951).
5. H. Miyazaki, Combined free and forced convective heat

transfer and fluid flow in a rotating curved circular tube, *Int. J. Heat Mass Transfer* **14,** 1295–1309 (1971).
6. H. Miyazaki, Combined free and forced convective heat transfer and fluid flow in a rotating curved rectangular tubes, *J. Heat Transfer* **95,** 64–71 (1973).
7. L. Wang, Fluid flow and heat transfer in rotating curved channels, Ph.D. thesis, University of Alberta, Edmonton (1995).
8. A. Aziz, Perturbation methods. In *Handbook of Numerical Heat Transfer* (Edited by W. J. Minkowycz, E. M. Sparrow, G. E. Schneider and R. H. Pletcher), pp. 625–671. Wiley, New York (1988).
9. M. Van Dyke, Computer extension of perturbation series in fluid mechanics, *SIAM J. Appl. Math.* **28,** 720–734 (1975).
10. M. Van Dyke, Extended Stokes series: laminar flow through a loosely coiled pipe, *J. Fluid Mech.* **86,** 129–145 (1978).
11. M. Van Dyke, Extended Stokes series: laminar flow through a heated horizontal pipe, *J. Fluid Mech.* **212,** 289–303 (1990).
12. H. C. Topakoglu, Steady laminar flows of an incompressible viscous fluid in curved pipes, *J. Math. Mech.* **16,** 1321–1337 (1967).
13. S. N. Barua, Secondary flow in a rotating straight pipe, *Proc. R. Soc. Lond.* **A227,** 133–139 (1954).
14. L. Wang and K. C. Cheng, Flow in curved channels with a low negative rotation speed, *Phys. Rev. E* **51,** 1155–1161 (1995).
15. H. P. Greenspan, *The Theory of Rotating Fluids*. Cambridge University Press, Cambridge (1968).
16. Y. Mori and W. Nakayama, Convective heat transfer in rotating radial circular pipes (1st report, laminar region), *Int. J. Heat Mass Transfer* **11,** 1027–1040 (1968).
17. Y. Mori, T. Fukada and W. Nakayama, Convective heat transfer in rotating radial circular pipes (2nd report), *Int. J. Heat Mass Transfer* **14,** 1807–1824 (1971).
18. W. R. Dean, The stream-line motion of a fluid in a curved pipe, *Phil. Mag.* **5,** 673–695 (1928).
19. S. Goldstein, *Modern Developments in Fluid Dynamics*, Vol. 2. Oxford University Press, Oxford (1957).
20. K. Mansour, Laminar flow through a slowly rotating straight pipe, *J. Fluid Mech.* **150,** 1–24 (1985).